THE UNIVERSITY OF AUCKLAND
NEW ZEALAND
Te Whare Wānanga o Tāmaki Makaurau

Vulnerability of New Zealand pastoral farming to the impacts of future climate change on the soil water regime

Client report: (CC MAF POL_2008-21 (128-3))

30 June, 2008

Vulnerability of New Zealand pastoral farming to the impacts of future climate change on the soil water regime

Anthony Fowler

Simon Aiken

Kim Maree

Client report prepared for:

The Ministry of Agriculture and Forestry

(Sustainable Land Management and Climate Change Research Fund)

(CC MAF POL_2008-21 (128-3))

School of Geography, Geology, and Environmental Science
The University of Auckland
Private Bag 92019
Auckland Mail Centre
Auckland 1142

Contents

Executive Summary

It is now widely agreed that some of the most significant impacts of future climate change are likely to be associated with the hydrological cycle, including potentially significant impacts on the soil water regime. The importance of agriculture to the New Zealand economy means that any such impacts are important to us. Moreover, the most recent climate change scenarios developed for the New Zealand region suggest possible enhanced vulnerability in some regions, due to likely changes in the strength of prevailing winds, interacting with New Zealand's complex topography.

The orthodox approach to assessing potential climate change impacts is a "top-down" methodology, which uses a cascade of climate and biophysical models to assess impacts (i.e. climate → water resources → agricultural productivity). This methodology is limited by the fact that regional-scale uncertainties about climate change are very large, to the extent that realistic representation of them can result in even the direction of change being uncertain, or reversing when climate change scenarios are revised.

An alternative "bottom-up" approach is proposed here which focuses on the sensitivity of the soil water regime and associated pasture productivity to climate change – in effect addressing the "do we have a potential problem?" question prior to launching a complex (and expensive) full-scale climate change impact assessment. The research is a pilot study with three specific research aims: a) develop a generic methodology for preliminary assessment of the vulnerability of pastoral production to climate change; b) build a user-friendly software tool to implement that methodology, and; c) test both in a case study context (proof of concept).

Core to the methodology used here is the idea that the sensitivity of the soil water regime and pasture productivity to future climate change is best assessed within the context of natural climate variability. To facilitate this:

- Multi-decadal climate time series were used to drive a daily water balance model (DWBM) of near surface hydrology.
- Pasture productivity was calculated from modelled evaporation (excluding interception).
- The input time series were systematically perturbed to assess the sensitivity of soil dryness and pasture productivity to climate change.
- Mean sensitivity of soil dryness and pasture productivity were displayed as two dimensional 'response surfaces'.
- Climate change impact assessment was undertaken by superimposing simplified scenarios of future climate change onto these response surfaces.
- The significance of the potential impacts was then assessed by comparing the simulated impacts with inter-annual variability (caused by natural climate variability).

Much of the above methodology was implemented in the DWBM and the method and model were tested on a Hawke's Bay data set. That application highlighted the elegance of the underlying concepts and showed that useful results could be obtained very quickly. It was also useful in identifying several implementation issues.

It is concluded that the proposed 'bottom-up' methodology is appropriate. The methodology, and the specific DWBM implementation, can reasonably be used to assess the sensitivity of pasture production to climate change. Extension of the analysis to all New Zealand climate regions is recommended, following some specific refinements:

- Use of more sophisticated climate change scenarios that realistically envelop plausible future climates.

- Further development of the DWBM to simplify the end-user experience and reduce the potential for error.
- Explicit testing and refinement of the pasture production model.
- Integration of the pasture production model into the DWBM, to circumvent time consuming and error-prone manual steps.
- Integration into the DWBM of several other manual steps in the methodology.

++++++++++++++++++++++

List of abbreviations (excluding technical appendix)

Abbreviation	Explanation	Units (if applicable)
DM	Dry matter production	kg/ha
DWBM	Daily water balance model	
IPCC	Intergovernmental Panel on Climate Change	
P	Precipitation	mm
PE	Potential evaporation	mm
PE_g	Potential evaporation over grass	mm
AWC	Available water capacity	mm
SW	Soil water	mm
E_{ts}	Evaporation (excluding interception loss)	mm
E	Total evaporation	mm
T	Surface air temperature	°C
SWD	Soil water deficit	mm
SON	Spring (September, October, November)	
DJF	Summer (December, January, February)	
MAM	Autumn (March, April, May)	
JJA	Winter (June, July, August)	
SONDJFMAM	Growing season (September – May)	

Note: DWBM parameters are listed separately in Table A1.

1. Introduction

It is now widely accepted that some of the most significant impacts of future global warming are likely to be experienced through regional-scale impacts on the hydrological cycle. There is abundant evidence in the palaeoclimate record that relatively small past changes in climate have resulted in significant regional changes in hydrology[1] (Roberts 1998) and simulations of future climate using global climate models consistently show that significant impacts on regional hydrology are likely (Christensen et al. 2007).

The Fourth Assessment Report of the Intergovernmental Panel on Climate Change (IPCC 2007) is the current substantive summary of the state of climate-change science. The report highlights and confirms previous findings that some of the most significant impacts of global warming are likely to be associated with changes in the frequency and intensity of droughts and heavy precipitation. IPCC (2007) further notes that associated trends in the historical record consistent with theory and modelling are "likely" and that continuing future trends are "very likely" for heavy precipitation, and "likely" for droughts. The former is associated with a general intensification of the hydrological cycle and the latter with changes in atmospheric circulation as the planet's heat distribution systems adjust to an altered state.

New Zealand's climate is dominated by its geographical location and regional rainfall regimes are determined by several complex and inter-related processes, including air-mass climatology, prevailing winds, sea surface temperatures, and topography (Sturman & Tapper 1996). The fact that the mountain backbone straddles the prevailing winds results in sharply contrasting regional rainfall regimes that are particularly sensitive to any variation in atmospheric circulation. The complexity of relationships makes modelling climate change impacts challenging – evidenced by the fact that global climate models disagree even on the sign of change in precipitation for some seasons (Christensen et al. 2007). Critically, however, ensemble modelling and empirical downscaling research has clearly demonstrated that major changes in important rainfall-regime drivers are practically certain for the New Zealand region (MfE 2008), with probable significant impacts on the frequency and magnitude of dry spells and heavy rainfall events (e.g. Mullan et al. 2005, Sansom & Renwick 2007).

Any future climate change impacts on regional rainfall will flow through to the soil water regime and, from there, to potential impacts on agricultural productivity and the economy. Moreover, given the importance of regional atmospheric circulation drivers as determinants of regional climates, the nature of those impacts are likely to be spatially variable, to the extent that there may be regional 'winners' and 'losers'. Moreover, since the sensitivity of farming and the New Zealand's economy to climate variability has been repeatedly demonstrated (most recently by the widespread 2007-8 drought), assessment of regional sensitivity and of potential future climate change impacts can reasonably be seen as an ongoing research imperative.

The orthodox approach to assessing potential climate change impacts is a 'top-down' methodology, which uses a cascade of climate and biophysical models to assess impacts (e.g. global climate → regional climate (downscaling) → soil water → agricultural productivity). The 'global climate' component is relatively mature, with multiple scenarios of future anthropogenic trace gas emissions used to drive multiple runs (with different starting values) of multiple models. This gives a sound basis for assessing future climate at global through continental-scale, but there are significant problems at the regional scale that is typically of interest for climate change impact assessment. Regional-scale uncertainties are very large, to the extent that climate models may

[1] Perhaps the most notable is the impact of changes in the latitudinal distribution of solar radiation in the early to mid Holocene (ca. 6-10 thousand years ago), associated with cyclic orbital variations, which affected the strength of the monsoons and the position of the Inter-tropical Convergence Zone (greening the Sahara). There is also evidence of floods and droughts (e.g. active dune fields in North America) that are unprecedented in human recorded history.

disagree on the sign of projected changes in precipitation. A realistic representation of these uncertainties through to impact assessment can result in even the direction of change being uncertain, or reversing when climate change scenarios are revised. These issues are well known by the research community and typically lead to the insistence that forecasts are not possible and that the scenarios produced should be regarded as plausible climate futures.

Recognising that the future is unknowable (conjointly because of uncertainties about human actions and incomplete science) MfE (2008) recommends an initial screening phase in climate change impact assessment to identify the sensitivity of a specific activity to plausible climate change, in order to determine the merits of proceeding with a full (expensive) impact assessment. In essence this represents an alternative 'bottom-up' approach that allows end-users to address the "do we have a potential problem?" question prior to committing to investigating climate change scenarios and dealing with the associated uncertainties.

Although the 'bottom-up' approach has rather obvious merit, it may be neither simple nor optimal for end-users to undertake the required sensitivity analysis for some activities. Apart from the fact that the pertinent methodology and expertise may not be self-evident or to hand, it would clearly be inefficient for end-users to duplicate effort if a generic approach is feasible. Also, there would be national benefit in using the same methodology, since doing so would facilitate meaningful inter-regional comparison. Climate change impacts on the soil water regime and pasture productivity may be one such case, where the adoption of a common methodology is plausible. This paper develops such a methodology and tests it at one site (Hawke's Bay) thought likely to be particularly sensitive to future climate change.

The research presented here builds on previous work that developed the 'bottom-up' approach in the context of Auckland water resources (Fowler 1999). That research used daily historical records of precipitation (P) and potential evaporation (PE) to drive a daily water balance model (DWBM). Multiple model runs with adjusting P and PE were undertaken to determine the sensitivity of the soil water regime to climate change, represented as 'response surfaces'. An explicit future climate context was then provided by superimposing climate change scenarios onto the response surfaces. Figure 1 shows an example of the end result of these two analytical steps. The same approach is adopted here, but using multi-decadal input series of P and PE to drive the DWBM, in order to better represent decadal-scale variability of P. This is achieved by adopting the mean climatological PE approach advocated by Fowler (2002). A simple model of pasture productivity is used to link soil water hydrology with pasture productivity.

Figure 2 is an overview of the over-arching research framework within which this pilot study sits. For any site the DWBM is driven by daily P and PE time series, the latter based on the climatological PE concept (Section 2.2). It is anticipated that pasture productivity may be calculated using a pasture growth model driven by multi-decadal time series of daily soil water content and evaporation (output from the DWBM), observed daily temperature, and relevant solar variables (e.g. day length and azimuth angle). However, for this pilot study a simpler pasture production model is used, based solely on computed evaporation. (Section 2.3).

The specific aims of the pilot study are to:

1. develop a generic methodology;

2. build an end-user-friendly DWBM software tool to assist end-users to implement the methodology, and;

3. undertake a 'proof of concept' application at one site (Hawke's Bay).

Further work will be required to refine the tools (especially the pasture production model) and to extend analyses to the whole of New Zealand.

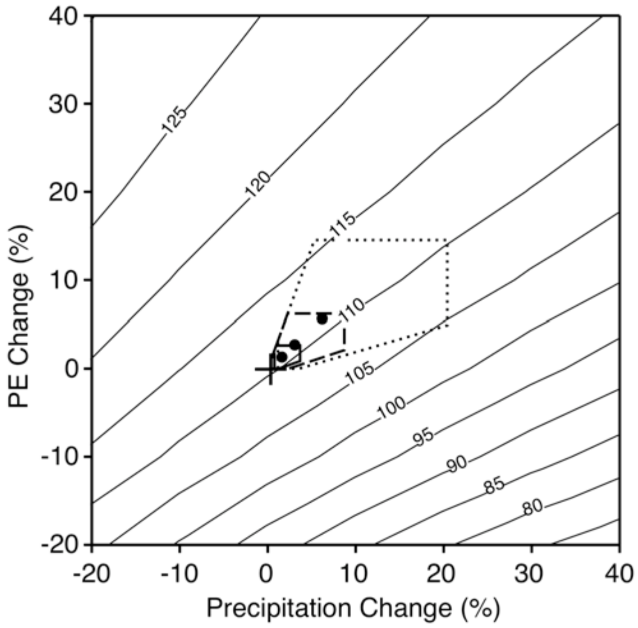

Figure 1. Example response surface, showing the sensitivity of mean summer soil water deficit (isopleths in mm) for an Auckland site to conjoint changes in precipitation and potential evaporation (PE). Superimposed on the response surface are climate change scenario best estimates (dots) and uncertainty envelopes for 2020, 2050, and 2100. Modified after Fowler (1999).

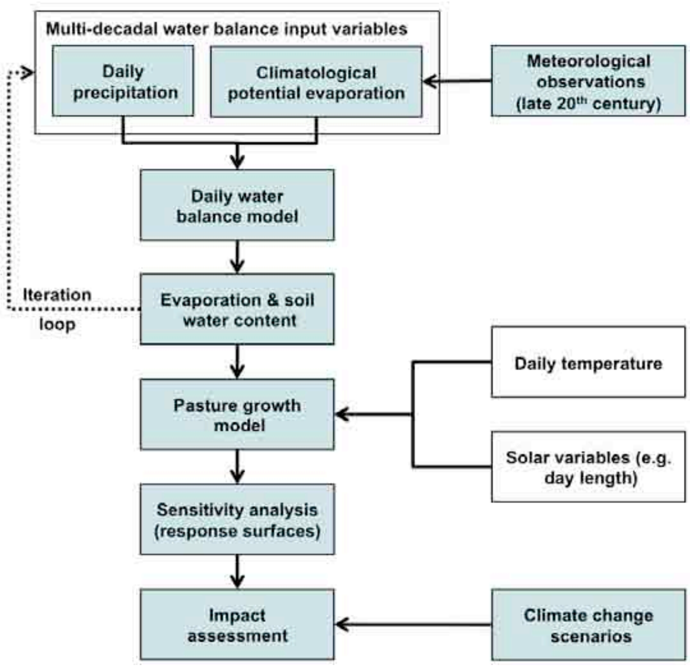

Figure 2. Research framework for analysis at a single site. White boxes represent components that are not implemented in the pilot study. The iteration loop refers to multiple runs of the DWBM with incremental adjustments to precipitation and potential evaporation, required to produce the sensitivity analysis response surfaces.

2. The analytical toolkit

2.1. Daily water balance model (DWBM)

The DWBM used here is the same as that used by Fowler (1999). The core soil water balance algorithms are unchanged, so direct comparison with previous work for the Auckland region (Fowler 1999, 2002; Fowler & Adams 2004) is possible. The program is written in the 'Java' programming language, enabling multi-platform deployment using a graphical user interface. A brief synopsis of the DWBM follows here, with a more detailed description presented in the Technical Appendix (Section 7.1).

- The DWBM operates with a daily iteration time step, and is driven by time series of P and PE (over pasture). P is corrected for characteristic under-measurement associated with deformation of the wind field around raingauges and evaporation losses.

- Effective rainfall reaching the soil surface is calculated using an empirical relationship between gross rainfall and interception loss for pasture. This separates evaporation of free water from leaf surfaces from transpiration.

- Effective rainfall is then partitioned between infiltration into the soil and surface runoff. The latter is usually small, requiring a wet soil and/or heavy precipitation.

- Soil water storage is defined in terms of available water capacity (AWC). There is facility to define some portion of AWC as an upper soil layer which fills and empties first.

- Infiltration is the only input to soil water storage. Outputs are slow drainage to groundwater, evaporation (excluding interception losses), and any surplus water once the soil has reached field capacity. Drainage is a function of soil water content. Evaporation is jointly controlled by PE (adjusted for any interception loss) and soil water content.

- Drainage, infiltration excess, and surplus fluxes pass through delay stores to produce 'runoff'. This is relevant here only in the context of verifying that the water balance partitioning is reasonable.

For the purpose of this research, three significant additions have been made to the model:

1. A graphical user interface has been added (Figure 3). This was done to add flexibility and speed to model setup and calibration, and to provide an immediate visual representation of the soil water balance simulation. It also presents the model in a user-friendly form to potential end-users, hopefully facilitating adoption.

2. Facility for multiple runs of the model has been added in order to automatically generate the output needed to produce response surfaces, such as that shown in Figure 1.

3. Additional summary output files related to evaporation fluxes are produced. These are used to model pasture productivity (external to the DWBM).

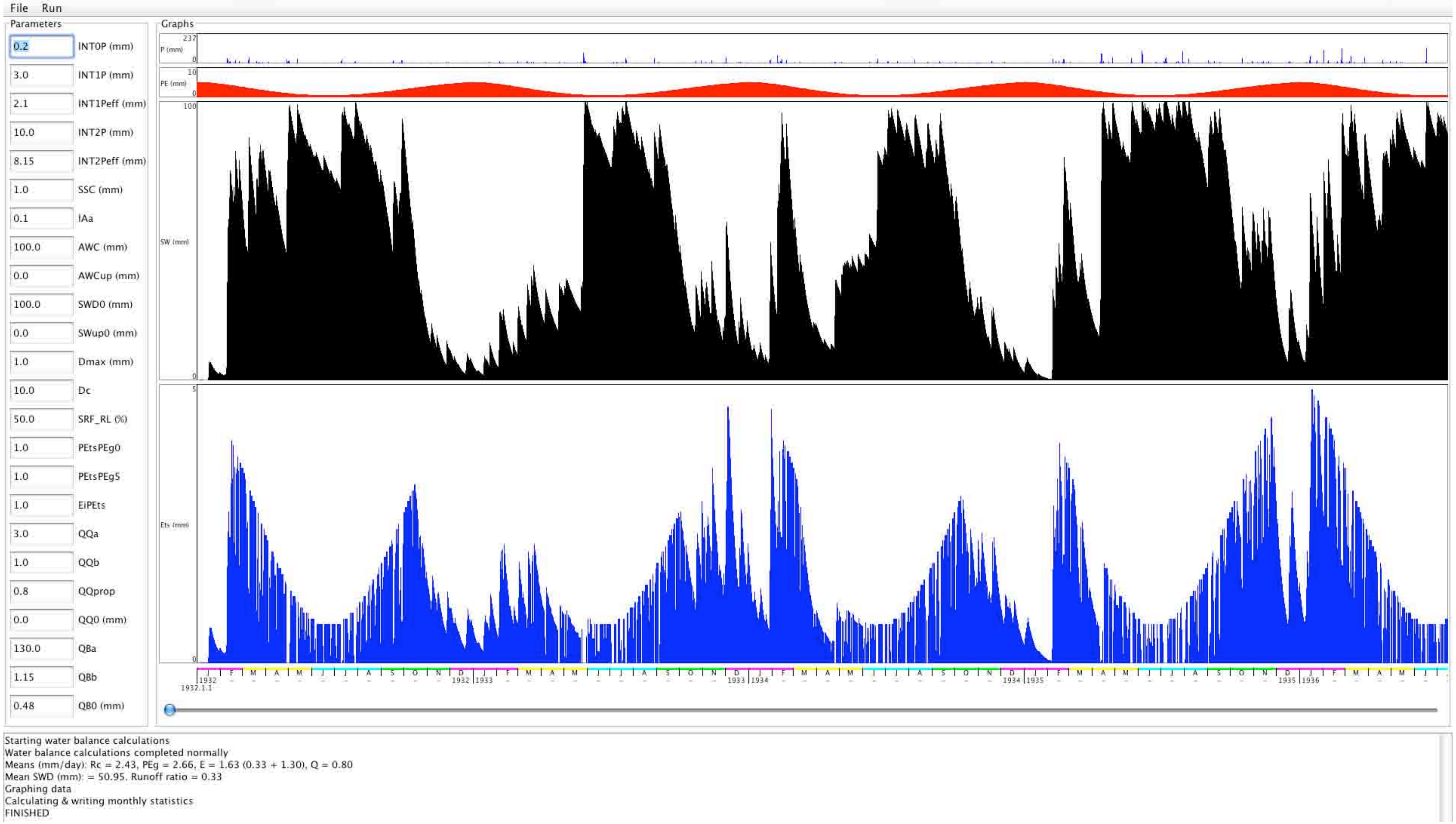

Figure 3. Graphical user interface for the DWBM. Model parameters and starting values for stores and fluxes are accessed through editable text fields (left panel) or can be read from (and written to) a text file. See Section 7.1 for a detailed explanation of parameters. The graphs show the daily results (mm) for the first few years of the simulation (P is rainfall, PE is potential evaporation, SW is soil water, Ets is evaporation, excluding interception loss). The lower panel is a text field used to inform the user of progress and to display simple summary statistics. Multiple simulations required to produce response surfaces are initiated through the 'Run' menu, but no graphical representation of the output is provided in this version of the model.

2.2. Long-term soil water balance modelling

Natural climate change on inter-annual through decadal time-scales (e.g. El Niño – Southern Oscillation and the Inter-decadal Pacific Oscillation) is critical for agriculture, especially in the context of the frequency and magnitude of regional droughts and wet periods. Experience with dealing with natural variability provides a useful reference for assessing the significance of projected changes in climate, and may provide useful temporal analogues for future conditions[2]. Moreover, because climate change associated with anthropogenic forcing is expected to be superimposed on natural climate change, any assessment of future impacts should sensibly proceed in the context of natural variability.

Accommodating natural climate variability could be achieved in the present context by running soil water balance simulations over a sufficient period of time (say 30+ years) to capture key elements of natural variability. This is problematic though because, although New Zealand has numerous rainfall records covering several decades and representing all climate regions, the data required to calculate PE is much more limited in both space and time. This is particularly the case for energy-based approaches to PE calculation, which require variables such as net radiation, wind, and humidity. Net radiation is a critical variable in these approaches, but it is rarely observed, and even observations of shortwave radiation are generally available at decadal-scale at best and for only a few locations. It is therefore necessary to resort to cruder alternatives, such as empirically-based measures (e.g. temperature-based relationships), pan evaporation, or semi-empirical approaches which retain the sophisticated equations, but use empirical relationships to derive the required variables (e.g. observations of sunshine hours or cloudiness to derive the radiation term). Stochastic approaches could also be used to generate long synthetic time series based on statistics derived from the limited observational record, but this approach may not adequately incorporate multi-decadal-scale natural variability.

Calder et al. (1983) compared the performance of soil water balance models using different levels of complexity in the treatment of PE and soil hydrology at grassland experimental sites in the United Kingdom. Contrary to expectations, some of the best results were obtained using a climatological value for PE, derived for a single central United Kingdom site. In essence, the daily water balance is calculated using observed precipitation, but using an estimate of PE that is a simple function of Julian Day (e.g. the value for 23 May is the same each year), derived from available short-term records. The rationale is that PE is an inherently conservative variable that is seasonally highly predictable. If a climatological estimate is used in the water balance, errors will tend to cancel out, so that calculated variables, such as soil water and runoff are similar to what would be obtained using PE values derived from daily meteorological observations.

Andersson and Harding (1991) obtained similar results to Calder et al. (1983) for two Swedish grassland sites, and in fact consistently superior results using climatological PE for six United Kingdom and Swedish forest sites. Porteous et al. (1994) came to similar conclusions about the merits of using climatological PE in a study of four New Zealand North Island grassland sites. Calder (1997) noted that the insensitivity of soil water balance modelling to the method used to calculate PE is a common feature identified in several studies.

Fowler (2002) confirmed the utility of the climatological PE method, even under relatively extreme conditions (Figure 4). Although the best results were obtained where a PE reduction was applied to account for PE suppression on rain days, the improvement was minor compared to simpler methods, leading to the conclusion that a simple monthly function should suffice.

[2] For example, historical droughts and wet periods may be useful analogues for future average conditions under a scenarios of significantly reduced or increased rainfall.

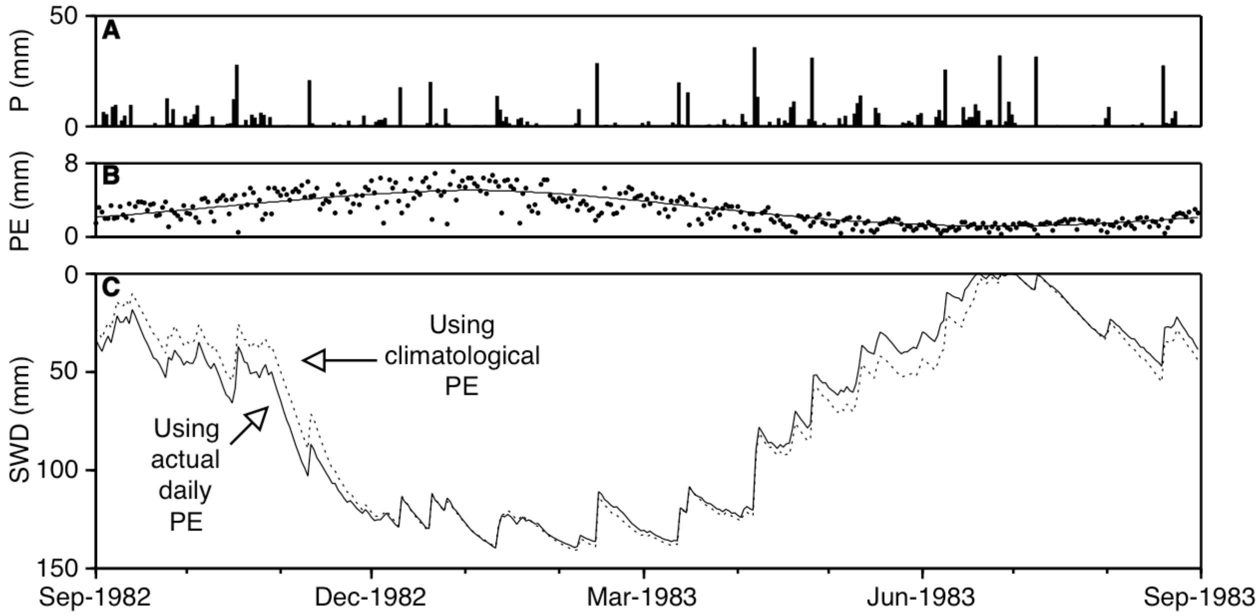

Figure 4. Comparison of DWBM simulation results (Sept-1982 – Aug-1983) using actual and climatological PE estimates. (A) Daily rainfall input common to both model runs. (B) Actual daily PE (dots) and climatological PE (curve) used as input to the two DWBM simulations. (C) Modelled soil water deficit (SWD). Results are for Auckland pasture. Note that this is the *worst* result obtained for 13 simulation years. Modified after Fowler and Adams (2004).

Adopting the climatological PE method here allows simulations to be run for the length of the available P record. Importantly, it means that analyses can be run for all New Zealand climate regions (though not for this pilot study).

2.3. Relating pasture production to the soil water regime

It has long been known that there is a close relationship between transpiration and crop dry matter production (DM). Chang (1968) pointed to the classical experimental work of Briggs and Shantz (1913) which showed very strong linear relationships between water transpired and DM of oats and barley. He also noted that reviews of studies on the relationship between transpiration and DM for 10 crops by De Wit (1958) and Arkley (1963) showed a linear relationship in every instance. Subsequent experimental studies have repeatedly shown a strong relationship between transpiration and the productivity of numerous agricultural crops, to the extent that DM can reasonably be considered to be proportional to transpiration, at least to a first approximation (McAneney and Judd 1983) – although the relationship only holds for actively growing plants and can breakdown if other unfavourable environmental conditions become critical (Chang 1968).

Building on the McAneney and Judd (1983) conclusion, Moir et al. (2000) investigated if New Zealand pasture DM can be successfully modelled as a function of evaporation. They used a simple water balance model to simulate total evaporation (E) from pasture and related cumulative growing-season DM to cumulative E at several sites in the Wairarapa (Figure 5). They identified strong linear relationships for all sites and attributed inter-site differences in regression line slopes to site differences in soil fertility. DM ranged from 11–19 kg/ha/mm of evaporation.

The strength of the relationships identified by Moir et al. (2000) is considered sufficient to warrant using such an approach to simulate the sensitivity of pasture DM to climate change and to investigate potential climate change impacts (at least in terms of the pre-screening context of this pilot study). Because the relevant evaporation information is readily available as DWBM output, multi-decadal application of the model at numerous New Zealand locations is feasible. This has significant benefits in terms of encompassing a realistic range of natural climate variability, and also in terms of transportability of the method.

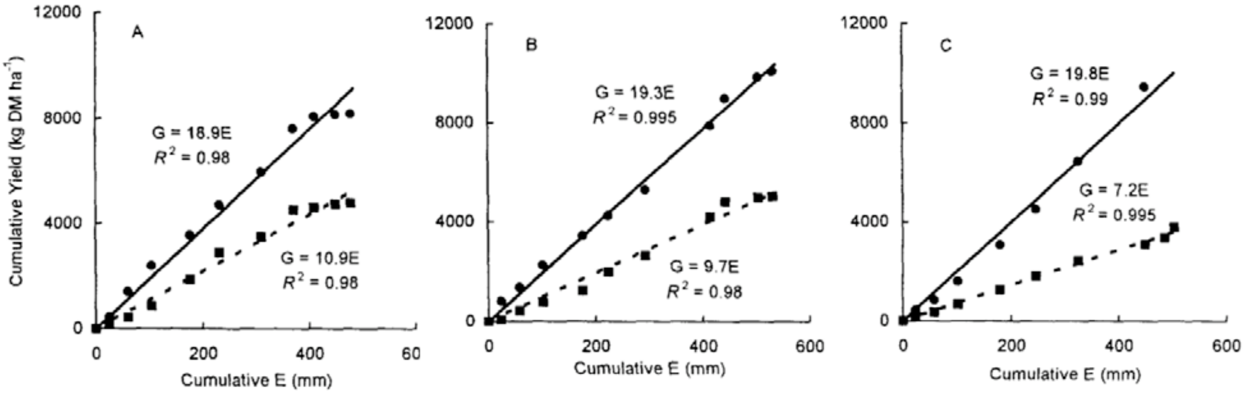

Figure 5. Relationships between cumulative evaporation (E) and cumulative pasture DM (August 1993 – April 1994) for six Wairarapa sites. Dot and square symbols denote high and low fertility sites respectively at Whareama (A), Gladstone (B), and Mauriceville (C). Source: Moir et al. (2000) (rearranged).

The DWBM used here is somewhat more sophisticated than that used by Moir et al. (2000). Of particular note is the fact that, because interception losses are modelled separately, there is additional flexibility in how the relationship between evaporation and pasture DM is constructed. We have chosen to exclude interception losses from our relationship, on the grounds that the previously identified empirical relationships for DM are more correctly with transpiration than with total E.

For the purpose of sensitivity and impact assessment (Section 4), we assume a mid-range value of 15 kg DM/ha/mm evaporation. This is probably somewhat low, given that the 11–19 kg range given by Moir et al. (2000) is derived for evaporation inclusive of interception. However, because the pasture productivity model is a simple linear scaling of evaporation, the value selected is of little consequence (results can be scaled up or down to account for different soil fertilities).

3. Historical climate data

3.1. Site selection

Hawke's Bay and the Canterbury Plains were considered as potential sites for the pilot study. Both are low rainfall regions in the lee of the main divide and both have significant current water resource issues. This means that they are both likely to be highly sensitive to the sort of changes in atmospheric circulation that climate models are suggesting (e.g. strengthening of the prevailing westerlies).

Monthly data from several climate stations at each site was accessed from the national climate database, then analysed to assess the quality of the data. The aim was to drive the DWBM using recent data, preferably with an unbroken daily record for more than 30 years. The Napier sites assessed were Napier Airport and Nelson Park. The main Christchurch sites were Christchurch Airport and Highbank Power station. This preliminary data screening lead to the selection of Hawke's Bay as the pilot study region.

3.2. Regional hydroclimatology

Hawke's Bay is sheltered from prevailing westerly winds by mountain ranges. This results in a relatively low mean annual rainfall (~1000 mm) and one of the lowest number of rain days in the North Island. The region is characterised by a relatively mild wind regime, high sunshine hours (mean ~2280 hrs/yr), and mild to warm surface air temperatures (T) with a consistent diurnal range of about 10 °C (Figure 6). However, significant exposure to easterly influences, in particular the erratic occurrence of cyclonic storms, results in a more variable precipitation regime than many New Zealand districts (de Lisle and Patterson, 1971).

Figure 6 shows the seasonal distributions of Napier mean P, T, and PE (Sep–Sep year), with associated implications for the soil water budget. The latter were derived from a DWBM simulation, assuming a soil water storage capacity of 100 mm. Figure 6 shows that, for a (purely hypothetical) average year:

- Soil water content is close to capacity by the end of winter (low SWD).
- Plant utilization of soil water begins in earnest in September and continues rapidly to November, depleting about 74% of available water. Depletion then slows over the two peak PE month (December, January), due to soil water content limitations on E. SWD typically peaks in January.
- Increasing P and declining PE from February starts a six month period of soil water recharge through to mid-winter. This is slow in February and March, due to PE being greater than P (but E < P), with the bulk of the recharge in May and June (P > PE by a factor of 2–4).
- Surplus (loosely equivalent to runoff) peaks over the winter months, due to a combination of relatively high P and minimum SWD. It then declines in concert with rising SWD to a low in January before beginning to rise again. The notable step-up in June and July is associated with SWD approaching zero, with an associated increase in drainage of water from the soil.

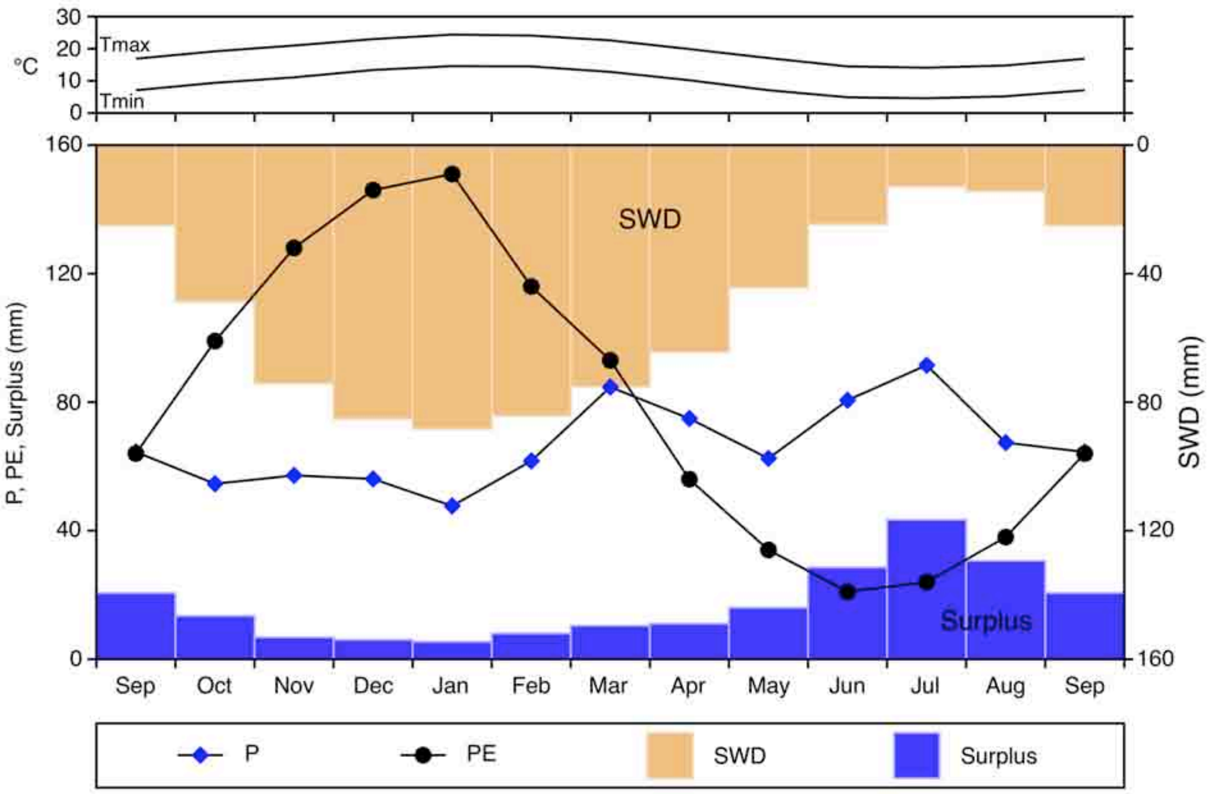

Figure 6. Napier hydroclimatology. Top: monthly mean minimum and maximum surface air temperatures (Tmin, Tmax) for Nelson Park (1971–2000). Bottom: monthly mean P and PE for Nelson Park (1941–1984) and DWBM-simulated soil water deficit (SWD) and surplus for a soil with an AWC of 100 mm. Sources: Nelson Park data from the National Climate Database (cliflo.niwa.co.nz) and NZMS (1986).

3.3. Construction of a daily historical rainfall and potential evaporation data set

Homogeneity assessment of Napier climate stations led to the selection of Nelson Park as the reference site. Several months of missing data from July to September 2005 were infilled using Napier Airport data (Napier Aero AWS) (Figure 7).

Daily rainfall data for Nelson Park and Napier Airport were accessed from the National Climate Database, giving a dataset extending from 1932 to early 2008. Gross daily rainfall was corrected for wind-field deformation and evaporation losses following Sevruk (1982). This increased annual rainfall by about 10.1% (6.7% for wind-field deformation plus 3.4% for evaporation losses).

Daily PE values were based on climatological PE, as described in Section 2.2. Figure 8 shows the method applied to Napier, using monthly mean PE from NZMS (1986).

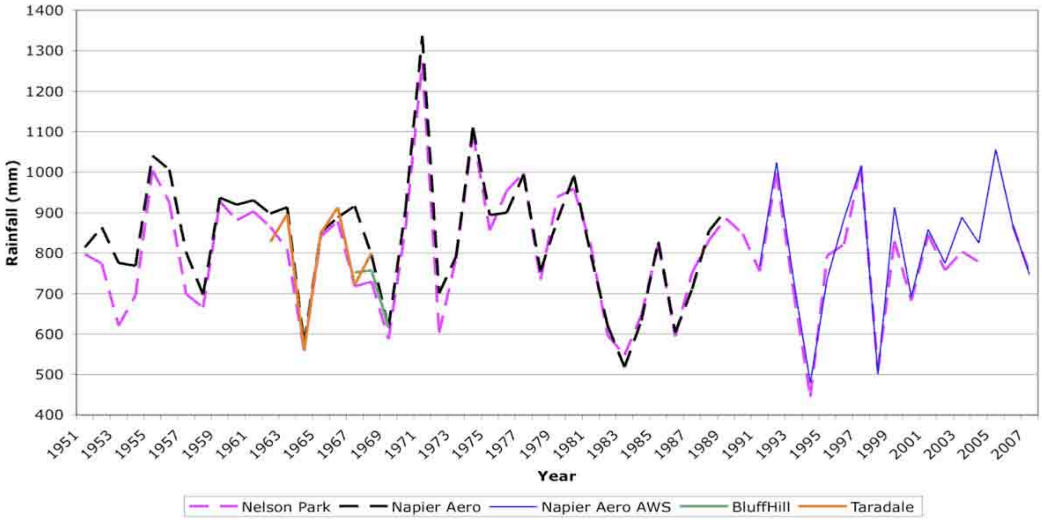

Figure 7. Annual rainfall recorded at several Napier sites (1951–2008).

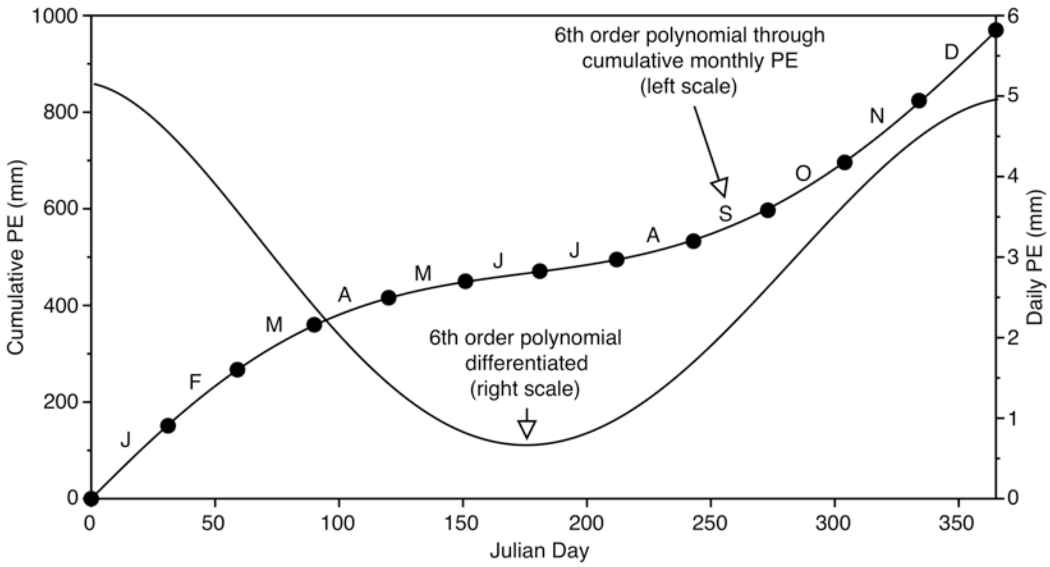

Figure 8. Calculation of climatological PE values from monthly mean PE for Napier. Monthly PE data from NZMS (1986).

4. Sensitivity and impact assessments

4.1. Overview of daily simulation results

Figure 9 shows DWBM simulation results for July 1981 through June 1983. The first half of this period was a fairly typical 12-month period (P = 914 mm). Simulated soil water content (SW) is close to capacity on 1 July 1981 and stays close to that through to the end of August. Because potential evaporation (PE_g) is low over winter, the simulated evaporation flux on rain days is dominated by interception losses (not shown in Figure 9). On dry days E_{ts} (predominantly transpiration) is close to the PE_g rate. As PE_g increases from September through to January, the soil dries and, from about the beginning of October, E_{ts} is consistently less than PE_g. The downward trend in soil water is episodically reversed by five storms in October, November, and December, with corresponding increases in E_{ts}. However, a seven week dry period from the last week of December is sufficient to essentially deplete soil water by mid-February, with negligible E_{ts} over this period. Frequent moderate rainfall in March and April, combined with declining PE_g , results in soil water replenishment by the end of April, with a recovery in E_{ts} rates rather earlier.

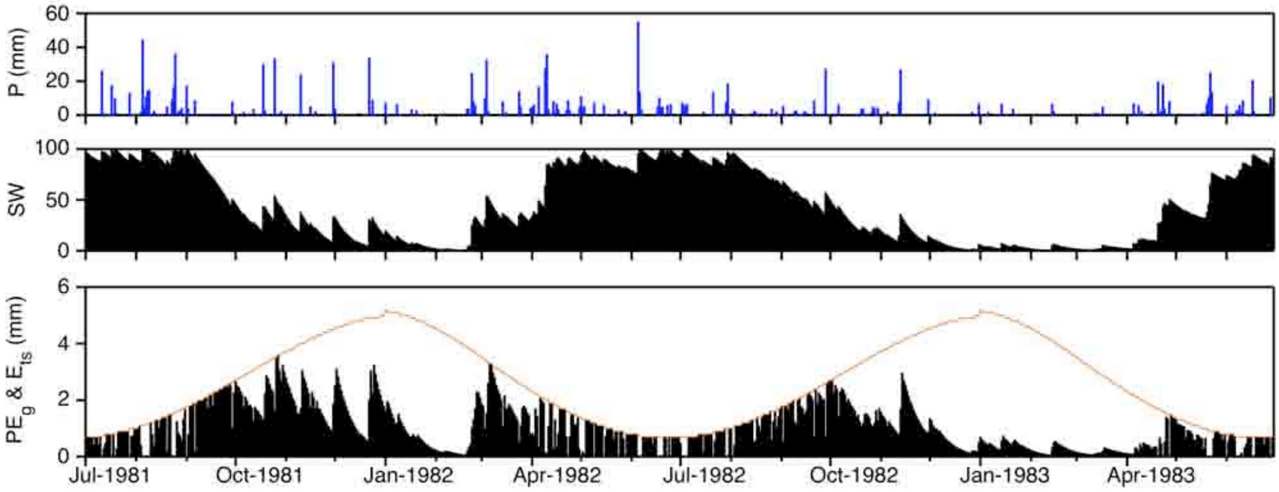

Figure 9. DWBM daily simulation results (July 1981 to June 1983). Top: daily precipitation (P). Middle: soil water content (SW). Bottom: climatological potential evaporation (PE_g, thin line) and actual evaporation excluding interception (E_{ts} , bars).

A significant El Niño occurred in 1982-83, bringing drought to several New Zealand regions, including Hawke's Bay (July 1982 to June 1983 rainfall about half of normal). Impacts on the simulated soil water regime and E_{ts} were severe (Figure 9). For example, soil water deficits were very high for the six months from mid-October through to the end of April, two months longer than in the near-normal 1981-82 season, described above. For the seven months from October to April, simulated E_{ts} was only 20% of potential, half that for the previous growing season.

Because the DWBM simulations are run over multiple decades, events such as the 1982-83 drought can be given a decadal-scale climate variability context. For example, Figure 10 shows that 1982-83 was one of two low 'outlier' years, with cumulative E_{ts} over September to May about 60% of the mean. In contrast, 1935-36 was a high E_{ts} year with a cumulative total about 50% above the mean. Because the pasture growth model used here is simply a linear scaling of E_{ts} , these results are also indicative of decadal-scale variability in total pasture production.

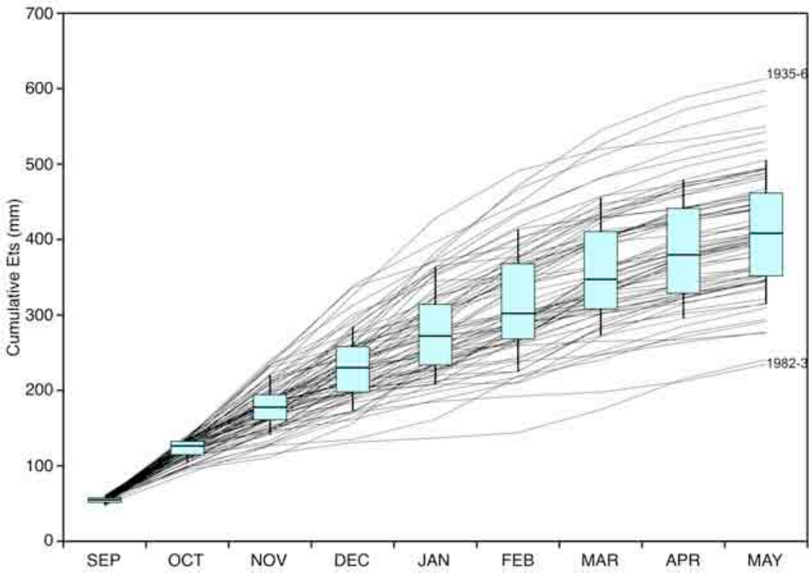

Figure 10. September to May cumulative transpiration (1932-2007), simulated by the DWBM. Thin lines are separate growing seasons. Box-and-whiskers plots show monthly medians (middle line) and the inter-quartile and inter-decile ranges (boxes and whiskers respectively).

4.2. Sensitivity of DWBM output to parameter values

Analysis of the sensitivity of key DWBM output variables to model parameter values is detailed in Section 7.3. Noteworthy findings are as follows:

- Adjusting interception parameters affects the relative contributions of E_i and E_{ts}, but has only a minor impact on total E.
- Adjusting infiltration parameters has relatively minor impacts on E_{ts}, with associated small impacts on soil water and runoff.
- Model output is most sensitive to changes in AWC.
- Including a pseudo upper soil layer has only a modest impact.
- Model output is insensitive to adjustments to drainage parameters.
- Output is moderately sensitive to the parameter controlling the soil dryness at which E_{ts} declines below the potential rate (SRF_RL).
- Sensitivity to explicit vs. pooled modelling of interception is complex. Pooling reduces E in all months, with reciprocal impacts on runoff, and widens the inter-seasonal range. Impacts are smallest over the growing season.

Based on the results of the sensitivity analysis, four sets of parameter settings were selected for subsequent analysis. These are:

1. Baseline analysis (default parameter values as detailed in Table A1).
2. AWC = 200 mm (double soil water storage capacity). Other parameters same as baseline.
3. SRF_RL = 20% (E_{ts} declines below the potential rate at relatively low SWDs). Other parameters same as baseline.

4. SRF_RL = 80% (E_{ts} declines below the potential rate at relatively high SWDs). Other parameters same as baseline.

Results are reported in some detail for the baseline simulation, and for other simulations in terms of how they differ.

4.3. Sensitivity of the soil water regime to climate change

Figure 11 shows the sensitivity of seasonal mean SWD to conjoint percentage changes in P and PE_g for the 'baseline' run. The orientation of the SWD isopleths indicates relative sensitivity to changes in the two driving variables (graph axes), while their spacing indicates the scale of that sensitivity. For example, the <45° slope of most of the spring (SON) isopleths indicates that SON SWD is more sensitive to changes in PE_g than P (a 20% increase in P reduces mean SWD by 4.6 mm, whereas a 20% increase in PE_g increases it by 8.2 mm), while consistent isopleth spacing across the response surface indicates near-linear sensitivity of mean SWD to incremental adjustments to P and PE_g.

The mean SWD isopleths steepen and become more asymmetric in summer (DJF). The former indicates that changes in P are now more important, although the fact that the isopleth slopes are still predominantly less than 45° indicates that changes in PE remain slightly more influential. The asymmetry is a consequence of the much drier soil in DJF, which limits the capacity for further drying (higher SWDs) as P decreases or PE increases, but which provides scope for significant wetting up (lower SWDs) under the reverse scenario.

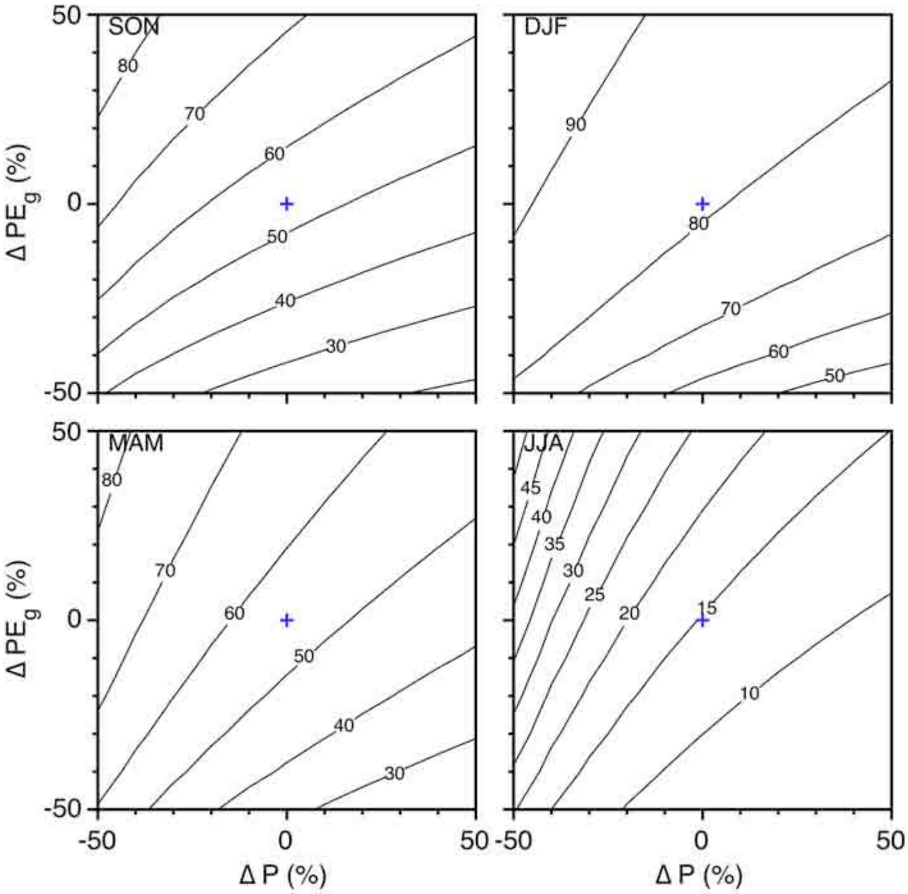

Figure 11. Response surface representations of the sensitivity of seasonal mean SWD (mm, isopleths) to conjoint change in P and PE_g. The '+' symbols denote the results for the DWBM run for unadjusted P and PE_g (1932-2007). Baseline run parameter values.

The return to mid-range SWDs in autumn (MAM) results in fairly even isopleth spacing and slopes of about 45°. This indicates that changes in P and PE_g are equally important and also a return to near-linear sensitivity of mean SWD to incremental adjustments to P and PE_g.

Much wetter soils in winter (JJA) reduce the scope for additional wetting up, resulting in another asymmetric response surface, but with a reversed pattern to the DJF case. Sensitivity to changes in P is stronger than to changes in PE_g, especially as P is reduced.

Few of the sensitivity *patterns* shown in Figure 11 were significantly different in any of the three alternative simulation runs (not shown). The main impact of doubling AWC to 200 mm was to reduce the asymmetry of the DJF and JJA response surfaces. Adjustments to SRF_RL resulted in predictable wetting (SRF_RL=20) and drying (SRF_RL=80) across seasons. Impacts were greatest in SON and MAM, but perhaps most significant in DJF (Figure 12), because in this case the impact is on soils at their driest.

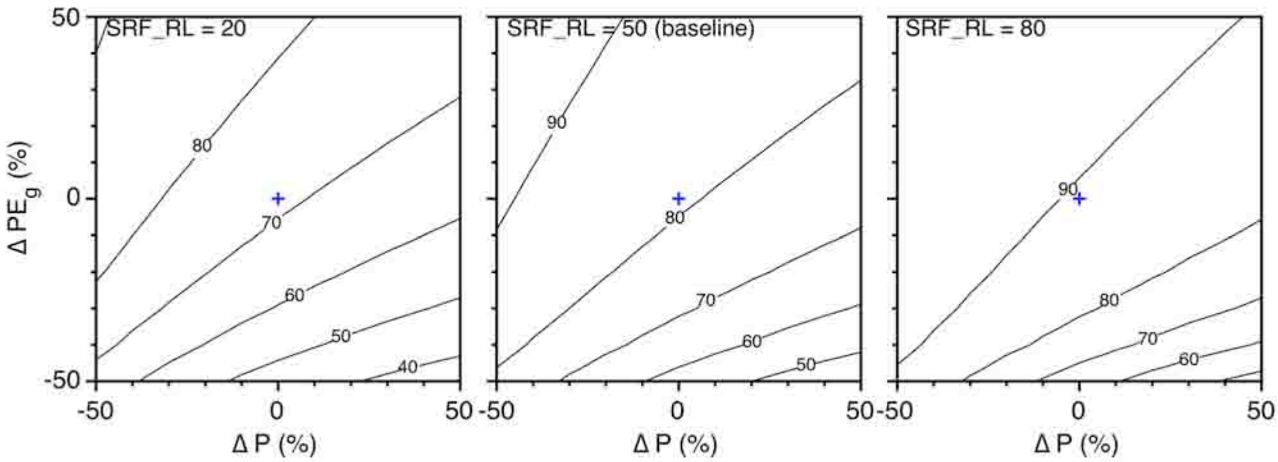

Figure 12. Sensitivity of DJF mean SWD (mm, isopleths) to conjoint change in P and PE_g, for alternative values for SRF_RL (other parameters set to baseline values). The '+' symbols denote the results for the DWBM run for unadjusted P and PE_g (1932-2007).

4.4. Sensitivity of pasture productivity to climate change

Recall that, based on results such as those presented by Moir et al. (2000) (Section 2.3), pasture production here is modelled as a simple linear function of E_{ts}. An indicative value of 15 kg/ha of DM production per mm of E_{ts} is used to produce the response surfaces plotted below, but with analysis constrained to the three primary growing seasons (SON, DJF, MAM). Total production across these nine months (SONDJFMAM hereafter) is also presented.

Figure 13 shows the sensitivity of pasture production to changes in P and PE_g, for the baseline simulation run. Note that the response surfaces are more complex than those presented for SWD and display more variable seasonal patterns. The anticipated increase/decrease in productivity as P and PE_g jointly increase/decrease is apparent, together with highly variable relative sensitivities. This variability relates to the evolving availability of soil water; pasture productivity is most sensitive to changes in P at times when soils are typically very dry (DJF), but to changes in PE when they are wet (JJA, not shown). Sensitivity is more evenly split between P and PE_g at intermediate soil water contents (SON, MAM), but relative importance varies substantially across the response surfaces, especially in SON. Finally, unlike SWD sensitivity, where the monthly results were characterised by a gradual transition in patterns across each season, the pasture productivity seasonal response surfaces 'hide' some abrupt transitions, to the extent that the seasonal response surface is sometimes uncharacteristic of any of the contributing month (see below).

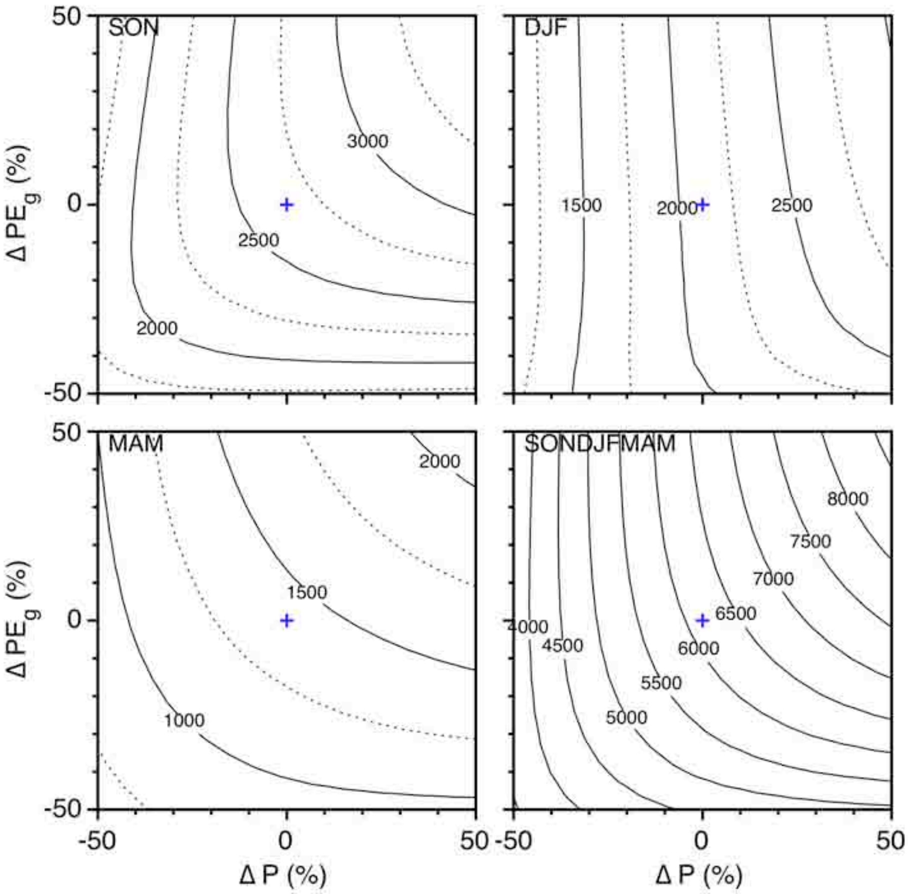

Figure 13. Sensitivity of seasonal mean pasture productivity (DM kg/ha) to conjoint change in P and PE_g. The '+' symbols denote the results for the DWBM run for unadjusted P and PE_g (1932-2007). Baseline run parameter values.

The response surface for SON is the most complex seasonal sensitivity pattern. Lower/higher P consistently results in lower/higher productivity throughout the -50% to +50% range modelled, but with increasing sensitivity as P declines and decreasing sensitivity as it increases. For example, a 20% reduction in P reduces productivity by 9.5%, but a 20% increase only increases it by 7.1%; relative differences that are amplified for larger changes in P. Sensitivity to PE_g changes is even more asymmetric. Productivity is reduced as PE_g decreases, but increases as PE_g is increased by 20% are only modest (3.8%) and negligible beyond that.

Inspection of the response surfaces for individual SON months (Figure 14) and the mean water balance (Figure 6) provides the explanation for the complex response surface pattern. SWDs are typically small in September, so E_{ts} is sustained at close to the potential rate for most of the month. September growth is therefore highly sensitive to changes in PE_g and insensitive to P changes. However, as SWDs increase through October and November, Ets becomes limited by available water and changes in P become the dominant control. Indeed, in November the relationship to changes in PE_g is reversed to weakly negative (for no change in P), caused by increased SWDs at the beginning of the month.

The DJF response surface shows a very simple relationship of insensitivity to PEg changes and strong sensitivity to P changes. The latter is strongest towards drying (isopleths more closely spaced) and is the strongest seasonal response pattern with ±20% P changes resulting in productivity changes of -17.8% to +15.5%.

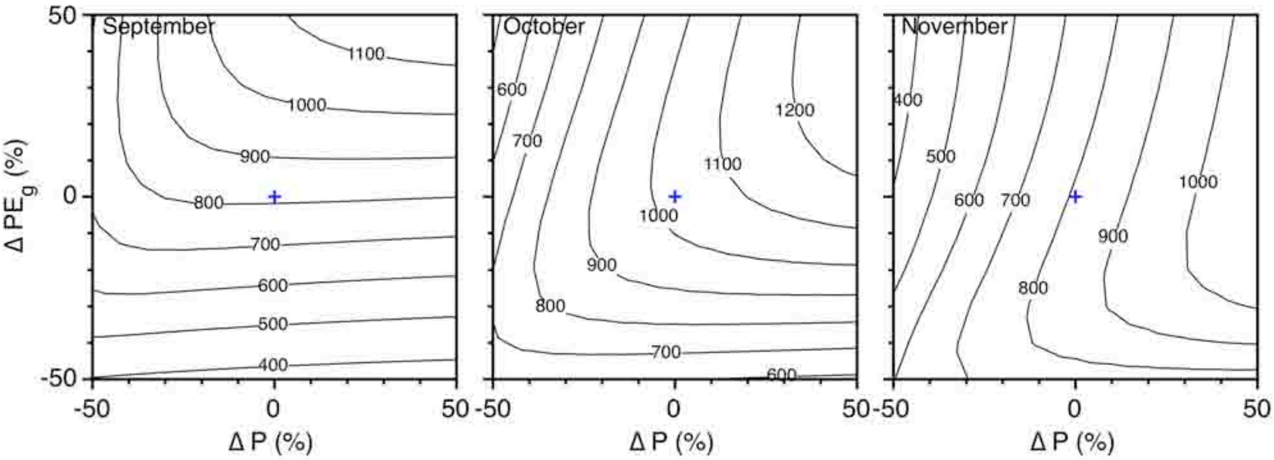

Figure 14. Sensitivity of monthly mean pasture productivity (DM kg/ha) for SON to conjoint change in P and PE_g. The '+' symbols denote the results for the DWBM run for unadjusted P and PE_g (1932-2007). Baseline run parameter values.

Production sensitivity is relatively subdued in MAM and roughly evenly weighted to changes in P and PE_g. Highest sensitivity is to reductions in both variables, with soil water availability again determining the pattern. This is essentially a reversal of the SON case, although more subdued because MAM wetting up of the soil is more gradual (Figure 6) and because production rates are lower.

The SONDJFMAM response surface shows whole of growing season sensitivity and is essentially the three seasonal response surfaces added together. The results show the potential for significant increases in productivity with conjoint and roughly equal increases in P and PE_g. Strongest sensitivity is to changes in P (predominantly vertical isopleths), especially if those changes are negative. For example, a 20% decrease in P results in a 12.8% reduction in productivity, which is not much affected by conjoint changes in PE_g. Note that this sensitivity pattern is dominated by the extreme relationship for DJF, although it is notably moderated by the SON and MAM patterns.

The seasonal response surface patterns in Figure 13 were not significantly affected by changing the threshold at which E_{ts} is reduced below the potential rate (Simulations #3 and #4 in Section 4.2). Total growing season production was impacted by ±4%, SON was most affected (due to higher soil water contents), and DJF was little affected.

Doubling AWC to 200 mm resulted in seasonal response surfaces with very similar patterns (Figure 15). One noteworthy change is in DJF where increases/decreases in PE_g result in small opposite impacts on productivity, compared with negligible impact for the baseline AWC of 100 mm. However, there are marked changes in the *scale* of the sensitivity responses, both within and between seasons. Most importantly, increased soil water storage capacity means that higher E_{ts} is sustained for longer during the drying cycle. September is little affected, because SWDs are low under either scenario, but about 30% higher E_{ts} rates in October and November result in a significant increase in SON pasture productivity. The effect persists through to January, resulting in a smaller increase in DJF productivity, but is unimportant from February through to September, leaving the MAM response surface little affected. SONDJFMAM pasture productivity increases by over 20%, almost all of which is contributed by the four months from October to January. Absolute production sensitivity is larger, but about the same in relative terms.

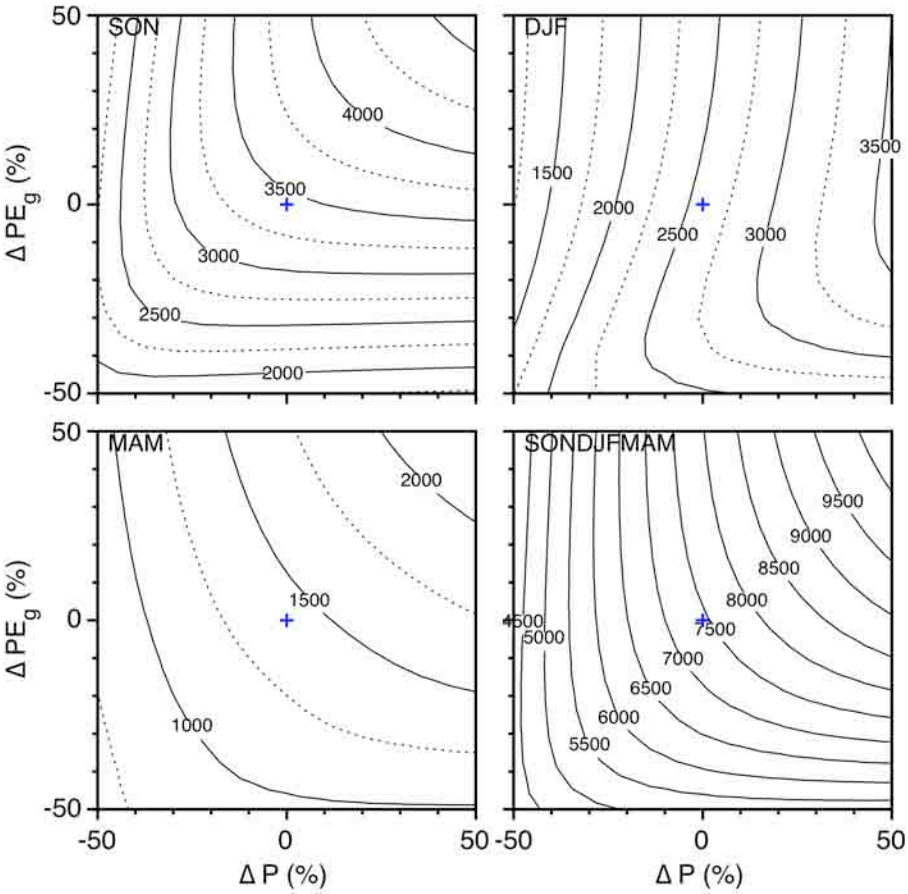

Figure 15. Sensitivity of seasonal mean pasture productivity (DM kg/ha) to conjoint change in P and PE_g. The '+' symbols denote the results for the DWBM run for unadjusted P and PE_g (1932-2007). AWC = 200mm. Baseline run values for other parameters.

4.5. Future climate change impact assessment

The response surfaces presented in the previous two sections are key tools for representing the sensitivity of system behaviour to possible climate forcing. However, in the context of potential future climate change impacts, they represent an incomplete analysis in two respects. First, the response surfaces do not provide the future context required to give the sensitivity analysis explicit relevance to end-users. It is all very well showing how pasture production might be affected by hypothetical changes to P and PE_g, but end-users need to know what subset of the response surface represents a plausible climate future. Second, the response surface approach used here focuses solely on changes in the mean. Because no information about inter-annual variability is incorporated, it is not possible to assess the significance of simulated changes in the mean, relative to natural climate variability. We therefore have no immediate way of knowing if a simulated change in mean pasture production of, say, DM 1000 kg/ha is within normal inter-annual variability or is outside the range of past experience.

Two additional analytical steps resolve the issues above. First, the future context is provided by superimposing scenarios of future climate change onto the response surfaces (e.g. Figure 1). Second, having done this we can then 'drill down' at critical points[3] on the response surface to extract and display the associated inter-annual variability. This is demonstrated below.

[3] The locations representing the best guess for future climate change and minimum and maximum impact points are the most obvious 'drill down' points.

Regional climate change scenarios for New Zealand were updated in 2008 (MfE 2008). The revisions were based on the global climate modelling work underpinning the IPCC Fourth Assessment Report (IPCC 2007) with empirical downscaling to the local level. The latter relied on historical relationships between (gridded) local climate and three indices of atmospheric circulation[4].

The late 21st century scenario for Hawke's Bay is for a best estimate increase in surface air temperature (relative to the late 20th century) of 2.2 °C, with an uncertainty range of 0.6–5.3 °C. Accounting for the 20th century warming trend over the 1932-2007 DWBM simulation period, and assuming a 2–4% increase in PE_g per °C (Fowler 1999), gives a best estimate of a 7.2% increase in PE_g (1.8–22.4% range). The best estimate for P change is -4% (-20–11% range).

The full future climate change scenario envelope is plotted as a simple box in Figure 16 on top of the SONDJFMAM pasture productivity response surface. Also plotted are symbols denoting the best estimate (dot) and two points on the envelope where production is relatively low and high (squares)[5]. From this simple overlaying of the scenario onto the response surface three key results immediately emerge:

1. *Best estimate is for minor impacts.* The best estimate changes in P (-4%) and PE_g (+7.2%) have inverse impacts on pasture productivity. Because production is markedly more sensitivity to changes in P than PE_g (steep isopleths), the net impact is a small decrease (<1%), even though the percentage change in PE_g is larger.

2. *Direction of change is uncertain.* The scenario overlay envelope indicates that uncertainties in projections of future climate flow through to either decreases or decreases in pasture productivity being plausible. There is also no clear preponderance in either direction.

3. *Plausible impacts are significant.* Plausible climate futures, represented by the limits of the envelope, indicate that mean pasture production may be impacted by up to about ±10%.

To give the results context in terms of inter-annual variability, the DWBM was re-run for each of the four points marked by symbols in Figure 16. Results for each year were extracted and cumulative probability plots produced (Figure 17). The significance of the simulated impacts was then assessed by comparing the cumulative probability plots for each of the three perturbed climate runs with that for the baseline run.

The cumulative probability plot for the baseline run indicates that simulated SONDJFMAM pasture production varies by about a factor of three, with a fairly even spread either side of the median (50% cumulative probability). The curve for the best-estimate simulation is almost identical, indicating that the minor impact shown for the mean by the response surface analysis carries through for the full range of natural variability.

The results for the low- and high-growth scenarios show that the ±10% impacts for mean production, previously noted, are fairly consistent through the range of low through high production years. Impacts for the low-growth scenario are somewhat larger for poor growth years (e.g. -16% at 10% cumulative probability) and lower for good growth years. Changes in productivity of ±10% represent impacts of about 350-900 kg/ha, much less than the baseline run inter-annual range (5683 kg/ha). Although this suggests that impacts may not be extreme, there are never-the-less some notable changes in frequency. For example, the middle arrow in Figure 17 shows that annual

---

[4] Zonally-averaged (160-190°E) pressure anomaly at the latitude of the grid point, Z1, M1 (MfE 2008, p. 124).

[5] The lower-left corner of the envelope is not chosen as the production minimum because the combination of maximum reduction in P and minimum increase in PE_g is considered implausible. More sophisticated analysis is required to refine the shape of the scenario envelope (e.g. Figure 1).

production was less than 6150 kg/ha in 50% of the 76 years from 1932-2007. This increases to 72% of years for the low-growth scenario and decreases to 35% for the high-growth scenario. At the extremes of the distributions the results suggest that drought impacts may be more severe (low-growth scenario) but also the possibility of about 5% of years with higher productivity than anything previously experienced (high-growth scenario).

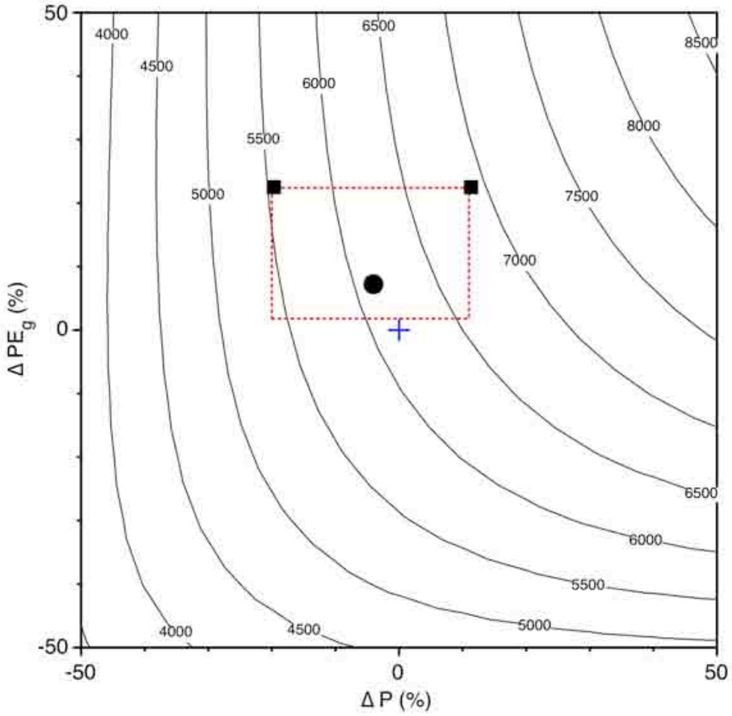

Figure 16. Potential climate change impacts on pasture productivity (SONDJFMAM) to conjoint change in P and PE_g. The '+' symbol denotes results for the DWBM run with unadjusted P and PE_g (1932–2007) and using default parameters. The dotted box envelops the range of uncertainty about future impacts to the end of the 21st century, based on MfE (2008) climate change scenarios. The dot is the best estimate and the two squares are 'best' and 'worst' case scenarios, in terms of pasture production impacts (see text for details).

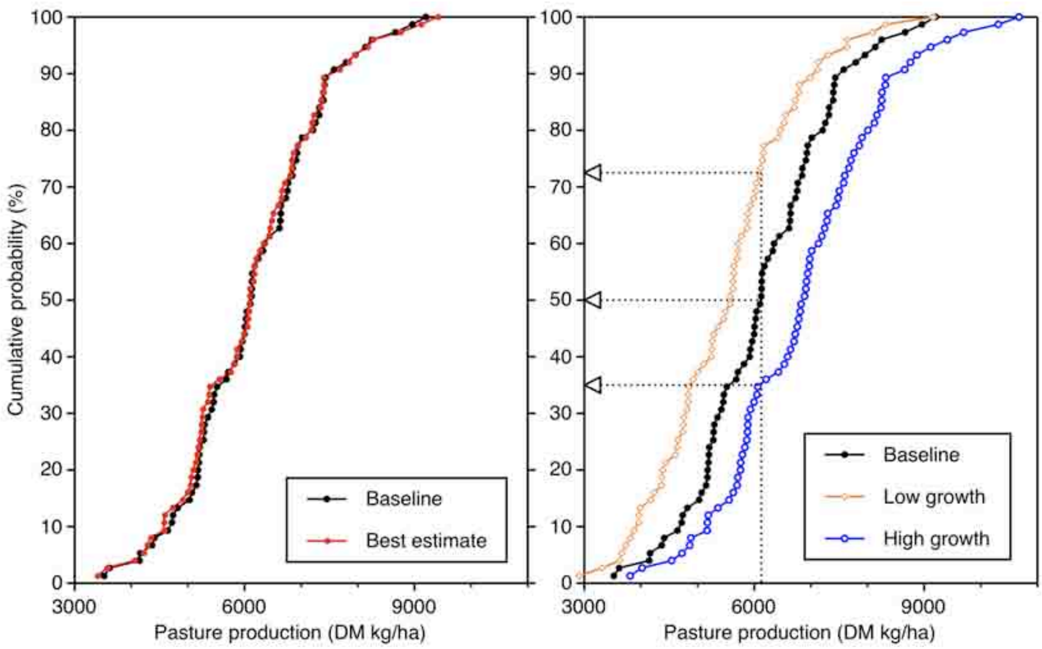

Figure 17. Cumulative probability plots of simulated SONDJFMAM pasture production (1932–2007) for the four points on the response surface (Figure 16) marked by symbols.

5. Discussion and conclusions

The aims of this study were to: a) develop a generic methodology for preliminary assessment of the vulnerability of pastoral production to climate change; b) build a user-friendly software tool to implement that methodology, and; c) test both in a case study context (proof of concept). The following three sections provide a summary and critique of these aspects. Section 5.4 details conclusions and recommendations for further developments.

5.1. Methodology

Core to the methodology used here is the idea that the sensitivity of the soil water regime and pasture productivity to future climate change is best assessed within the context of natural climate variability. To facilitate this, multi-decadal time series of observed P and climatological PE were used to drive a model of near surface hydrology. The input time series were then systematically perturbed, to assess the sensitivity to climate change of selected output variables. Pasture productivity was calculated from one of these (E_{ts}) and the sensitivity of the soil water regime and productivity to conjoint variation of P and PE_g were displayed as response surfaces. Climate change scenarios were superimposed on these response surfaces and the natural climate variability context was reintroduced for selected key points on the response surface (historical climate, best future estimate, impact range), using cumulative frequency curves.

The use of climatological PE is convenient, in that it allows the analysis to be extended to the extent of the reliable P record. We have argued that little is lost by resorting to climatological PE, but the methodology is not dependent on the use of climatological PE; alternative methods for calculating daily PE_g could be used, including sophisticated energy-balance methods for the last few decades. The likely trade off is length of record, and therefore the extent to which multi-decadal-scale variability in P (by far the most volatile variable) is accounted for.

At no point in this study have we dealt with the contentious issue of CO_2 fertilization impacts on either pasture productivity or on water-use efficiency (reducing PE_g as CO_2 concentrations rise). The former is outside the scope of the study, but clearly should to be considered in any full-scale impact assessment. The latter can be implemented by adjusting future climate change scenarios to account for uncertain but systematic reduction in PE_g as CO_2 concentrations rise. Because there are uncertainties about the scale of any fertilization impact[6], the climate change scenario envelope would need to expand (e.g. Fowler 1999). However, there seems little point adding such nuances until the scenario envelope is more refined than the simple box used here (Figure 16).

The impact assessment presented in Section 4.5 is a useful indicative demonstration of the methodology. The simplistic box shape used for the scenario envelope is sufficient for this purpose, but further analysis is required to realistically 'bound' the plausible future climate regime. Most importantly, the envelope should recognise the fact that changes in P and PE_g are not independent. For example, relatively large changes in P are usually associated with large changes in T (and hence PE_g). It follows that a simple box may include regions on the response surface that are not in fact plausible, on the basis of the suite of climate models used to develop the scenarios. Refining the scenario envelope to accommodate the above is not difficult, but neither is it a trivial task.

The pasture production results presented in this study were derived by a simple linear scaling of E_{ts}. The credibility of the pasture productivity sensitivity and impact assessments therefore rest, in turn, on the credibility of the modelling of E_{ts} and of the $E_{ts} \rightarrow$ pasture productivity relationship. Both are well founded in theory and empirical evidence, including for New Zealand, but neither is

[6] Uncertainty relates both to future concentrations of CO_2 and persisting uncertainty about the scale of any impact on transpiration under real-world conditions (vs. experimental studies).

explicitly tested in the Hawke's Bay case. To do so was beyond the scope of this study, but would be advisable if the methodology is to be applied.

5.2. Software

A key objective of this study was to develop a user-friendly DWBM software tool to implement the methodology. This was achieved by adding a graphical user interface to an existing (non-user-friendly) DWBM and adding some additional functionality. However, although the graphical user interface makes the DWBM much more useful for potential end-users, it remains a 'work in progress' is some respects. For example, there is no checking that selected parameter values are actually physically reasonable and no error checking code is included to warn users if parameter values or starting values are questionable. There is also no checking of the formatting of the input data files, potentially leading to inelegant exiting of the program in the event of number format errors. In short, it is assumed that the user knows what they are doing with little in the way of hand holding provided. Application of the model is straightforward and useful work can be done using default settings and simple adjustments to key parameters (e.g. AWC), but a reasonable degree of expertise is required to use the software efficiently and to its full capacity.

Related to the above, the DWBM is more complex than necessary. This is because it was developed for application at both field and catchment scale and for alternative vegetation types. One consequence is that the number of parameters and starting values used to define the operation of the model is much larger than necessary for the specific application here. For example, the last seven parameters shown on the left of Figure 3 ('QQa' through 'QB0') all relate to runoff and are essentially irrelevant. Also, three parameters ('PEtsPEg0, 'PEtsPEg5', 'EiPEts') exist to allow better representation of evaporation from non-pasture vegetation, and default to values of 1. For pasture-specific application of the model, extraneous parameters and starting values could be hidden, simplifying the end-user experience and reducing the scope for error.

The original intention was to integrate pasture production into the DWBM. This was abandoned for two reasons. First, when it became apparent that the pasture model would be a simple linear scaling of E_{ts}, there appeared to be little advantage in doing so (because E_{ts} could be simulated and pasture dealt with independently offline). Second, the possibility of future significant revision of the pasture model (Figure 2) meant that the modelling merits to adopting a modular approach were given priority. The downside of this decision is that the analytical steps subsequent to the modelling of E_{ts} are manual and error prone. They also require specialised graphing software to produce the response surface representations of sensitivity.

5.3. Proof of concept

Application of the methodology and tools to the Hawke's Bay highlighted the elegance of the underlying concepts and how quickly useful results could be extracted. However, it also exposed difficulties associated with data, scope for error (where expertise is lacking), and some problems associated with implementing some aspects of the methodology.

An important aspect of the work was the desire to utilise the maximum possible length of record, in order to achieve the best possible representation of multi-decadal-scale climate variability. Doing so exposes issues associated with data inhomogeneity and missing observations that are likely to require a reasonable level of expertise on the part of the end-user to resolve. Napier proved to be a reasonably 'clean' record in this regard, but other locations may well prove more problematic, requiring reasonable knowledge of the issues characteristically associated with climate data.

Expertise is also needed to 'build' the input data set for the DWBM. The algorithms used to correct P for under-measurement associated with wind-field deformation and wetting losses are not complex, and could easily be built into the DWBM, but the decisions that must be made regarding what adjustments are appropriate do require expertise and cannot be avoided. Some analytical work is also required to produce the climatological PE_g time series (Figure 8). This is relatively straight forward, but carries some risk of error and is one manual step that could be built into the DWBM.

The Hawke's Bay sensitivity analysis indicated that DWBM output relevant to pasture productivity is sensitive to a relatively small number of parameters (mostly those related to evaporation). This should simplify the end-user experience because most parameters can confidently be left at their default values. It also suggests that the user interface can be simplified by hiding irrelevant and unimportant parameters.

One very interesting result emerging from the Hawke's Bay case study is the contrast between the SWD and pasture productivity response surfaces (Figures 11 & 13). Whatever the reason for the differences[7], the results clearly indicate that inferences about pasture productivity based only on soil water status are likely to be flawed. For example, the DJF response surface in Figure 11 shows that SWD is more sensitive to change in PE_g than P and that any decrease in PE_g results in a decrease in mean SWD. In contrast, the DJF pasture productivity response surface in Figure 13 shows very low sensitivity to change in PE_g and that the wetter soils are associated with lower pasture productivity. This is because E_{ts} is more negatively affected by the reduced PE_g than it is positively affected by increased available soil water.

Superimposing future climate change scenarios onto the pasture response surface (Figure 16) is simple, elegant, and was found to be highly informative. Three significant conclusions immediately emerged, regarding minimal best-estimate impacts, uncertain direction of change, and significant plausible impacts. However, it is important to appreciate that the veracity of this approach depends, to a significant degree, on the quality of the superimposed scenario envelope. Unfortunately, going beyond the overly-simplistic box envelope used in Figure 16 would require fairly advanced knowledge of climate science, that may be beyond the capacity of most end-users.

Comparison of cumulative probability curves for selected points on the pasture productivity response surface (Figure 17) proved an effective way of giving the results context in terms of natural variability. It confirmed the response surface results that the best estimate for Hawke's Bay is for negligible change. It also showed that the best and worst-case changes of about ±10% are within a natural variability context of about ±50%. Further comparison of the cumulative frequency plots shows that a systematic shift in the frequency distribution change of this scale can result in notable changes in frequency of occurrence of different productivity levels, including putting 2–5 years per century outside the range of previous experience.

Finally, the case study application was invaluable in exposing the implications for the end-user of the decision to not incorporate pasture production into the DWBM, previously noted. The required manual calculation of pasture productivity through to the cumulative probability plots proved cumbersome and error prone. Calculation of the pasture productivity response surface (Figure 16) was fairly simple (spreadsheet to scale and sum E_{ts}, then a dedicated graphing package to plot the response surface), but deriving the cumulative probability plots (Figure 17) required the DWBM to be re-run with several modified input series, then further analytical and graphing work on the DWBM output files.

5.4. Conclusions and recommendations

Based on the results presented above, we conclude that the proposed 'bottom-up' methodology can reasonably be used to assess the sensitivity of pasture production to potential climate change impacts on the soil water regime. We recommend that the analysis be extended to all New Zealand climate regions, following refinements as listed below.

---

[7] The reasons relate to the influence of absolute upper and lower bounds in the case of SWDs, the fact that SWDs carry forward significant 'memory' of prior conditions, and the non-linear relationship between SWD and E_{ts}.

1. Climate change scenario should be more sophisticated. Scenarios should envelop only plausible climate futures and should be expanded to include all known sources of uncertainty.

2. The DWBM should be refined to simplify the end-user experience and reduce the potential for error.

    a. Irrelevant and unimportant parameters should be hidden.

    b. Less impenetrable parameter names should be used.

    c. Questionable parameter values should be flagged.

    d. File formatting should be verified (with elegant exiting of the program).

    e. Rainfall correction should be integrated.

    f. Climatological PE should be integrated.

3. The pasture production model should be tested (and modified if necessary).

4. The revised pasture production model should be integrated into the model (to circumvent time consuming and error-prone manual steps).

5. Other manual steps in the analysis, such as response surface plotting and derivation and plotting of cumulative probability curves, should be integrated into the DWBM. The latter should permit interactive interrogation of the response surface.

6. References

Andersson L, Harding RJ (1991) Soil-moisture deficit simulations with models of varying complexity for forest and grassland sites in Sweden and the U.K. *Water Resources Management*, 5, 25-46.

Arkley RJ (1963) Relationships between plant growth and transpiration. *Hilgardia*, 34, 559-84.

Aston AR, Dunin FX (1977) An empirical model for drainage from soil under rain-fed conditions. *Australian Journal of Soil Research*, 15, 205-210.

Baier W, Dyer JA, Sharp WR (1979). The versatile soil moisture budget. *Technical Bulletin 87*. Land Resources Research Institute, Ottawa.

Boughton, W.C. (1986). Linear and curvilinear baseflow recessions. *Journal of Hydrology (NZ)*, 25, 41-48.

Briggs LJ, Shantz HL (1913) The Water Requirements of Plants: I. Investigations in the Great Plains in 1910 and 1911. *Bureau of Plant Industry Bulletin*, 284. Washington D.C.: U.S. Department of Agriculture.

Calder IR (1997) Approaches for measuring and modeling soil moisture. In: Sorooshian S, Gupta HV and Rodda JC (eds.) *Land surface processes in hydrology: trials and tribulations of modeling and measurement*. Springer, Berlin. pp. 215-237.

Calder IR, Harding RJ, Rosier PTW (1983) An objective assessment of soil-moisture deficit models. *Journal of Hydrology*, 60, 329-355.

Chang J-H (1968) *Climate and Agriculture*. Aldine, Chicago.

Christensen JH, Hewitson B, Busuioc A, Chen A, Gao X, Held I, Jones R, Kolli RK, Kwon W-T, Laprise R, Magaña Rueda V, Mearns L, Menéndez CG, Räisänen J, Rinke A, Sarr A, Whetton P (2007) Regional Climate Projections. In: IPCC (2007).

de Lisle JF, Patterson DI (1971) The climate and weather of the Hawke's Bay region New Zealand. New Zealand Meteorological Service, Ministry of Transport, Wellington, New Zealand. *N.Z. Met. S. Misc. Pub. 115(5)*.

De Wit CT (1958) Transpiration and Crop Yields. Institute of Biological and Chemical Research on Field Crops and Herbage. Wageningen, The Netherlands, Vers-Landbouwk, Onder Z. No. 64-6-S Gravevage.

Fowler AM (1999) Potential climate change impacts on water resources in the Auckland Region (New Zealand). *Climate Research*, 11, 221-245.

Fowler A (2002) Assessment of the validity of using mean potential evaporation in computations of the long-term soil water balance. *Journal of Hydrology*, 256, 248-263.

Fowler A, Adams K (2004) Twentieth century droughts and wet periods in Auckland (New Zealand) and their relationship to ENSO. *International Journal of Climatology*, 24, 1947-1961.

IPCC (2007) *Climate Change 2007: The Physical Science Basis. Contribution of Working Group I to the Fourth Assessment Report of the Intergovernmental Panel on Climate Change* [Solomon, S., D. Qin, M. Manning, Z. Chen, M. Marquis, K.B. Averyt, M. Tignor and H.L. Miller (eds.)]. Cambridge University Press, Cambridge, United Kingdom and New York, NY, USA.

McAneney KJ, Judd MJ (1983) Pasture production and water use measurements in the central Waikato. *New Zealand Journal of Agricultural Research*, 26, 7-13.

McNaughton KG, Jarvis PG (1983). Predicting effects of vegetation changes on transpiration and evaporation. In *Water deficits and plant growth, Vol. VII: additional woody plant crops*, (ed. Kozlowski TT), pp. 147. Academic Press, New York.

MfE (2008). *Climate Change Effects and Impacts Assessment: A Guidance Manual for Local Government in New Zealand*. 2nd Edition. Mullan B, Wratt D, Dean S, Hollis M, Allan S, Williams T, Kenny G, and MfE. Ministry for the Environment, Wellington.

Moir JL, Scotter DR, Hedley MJ, Mackay AD (2000) A climate-driven, soil fertility dependent, pasture production model. *New Zealand Journal of Agricultural Research*, 43, 491-500.

Mullan B, Porteous A, Wratt D, Hollis M (2005) *Changes in drought risk with climate change*. Client Report WLG2005-23, NIWA, Wellington.

NZMS (1986). Summaries of water balance data for New Zealand stations: tables of evapotranspiration, wilting point deficit, runoff and soil moisture deficit for four selected available water capacities. New Zealand Meteorological Service, Ministry of Transport, Wellington, New Zealand. *N.Z. Met. S. Pub. 189*.

Parfitt RL, Joe EN, Cook FJ (1985a). Water use and pasture growth on Judgeford silt loam. *New Zealand Journal of Agricultural Research*, 28, 387 392.

Parfitt RL, Roberts AHC, Thomson NA, Cook FJ (1985b). Water use, irrigation, and pasture production on Stratford silt loam. *New Zealand Journal of Agricultural Research*, 28, 393 401.

Porteous AS, Basher RE, Salinger MJ (1994) Calibration and performance of the single-layer soil water balance model for pasture sites. *New Zealand Journal of Agricultural Research*, 37, 107-118.

Roberts N. (1998). *The Holocene: an environmental history* (2nd ed.). Blackwell, Oxford. Pages 112-126.

Sansom J, Renwick JA (2007) Climate change scenarios for New Zealand rainfall. *Journal of Applied Meteorology and Climatology*, 46, 573-590.

Sevruk B (1982) Methods of correction for systematic error in point precipitation measurement for operational use. *Operational hydrology report 21*, World Meteorological Organization, Geneva.

Sturman AP, Tapper NJ (1996) *The weather and climate of Australia and New Zealand*. Oxford University Press, Melbourne.

USDA (1972). *SCS National Engineering Handbook*. Soil Conservation Service, United States Government. Printing Office, Washington D.C.

7. Technical appendix

7.1. Detailed description of the daily water balance model

The DWBM (Figure A1) operates with a daily iteration time step, and is driven by time series of corrected rainfall (R_c) and potential evaporation over grass (PE_g). R_c is derived from recorded gross rainfall (R_g), corrected for wind-field deformation around the raingauge and evaporation losses, following Sevruk (1982). Corrections of upwards of 10% are typical, increasing with windiness, and therefore with elevation.

R_c is partitioned between interception (E_i) and effective rainfall (R_{eff}) reaching the soil surface. R_{eff} is calculated using an empirical relationship between R_{eff} and R_c (Figure A1, Inset A). This is based on the fact that there is usually a close relationship between gross rainfall and interception and that for most practical modelling purposes this relationship is sufficiently strong for interception loss to be derived from rainfall data alone, including for grass. The empirical relationship is defined by three hinge points (dots in Inset A), controlled by five parameters (#1 – #5 in Table A1), that form a crude curve. Interpolation line slopes should be less than 1:1 and steepen, as shown in Inset A. Beyond the last hinge point all additional rainfall is assumed to be effective.

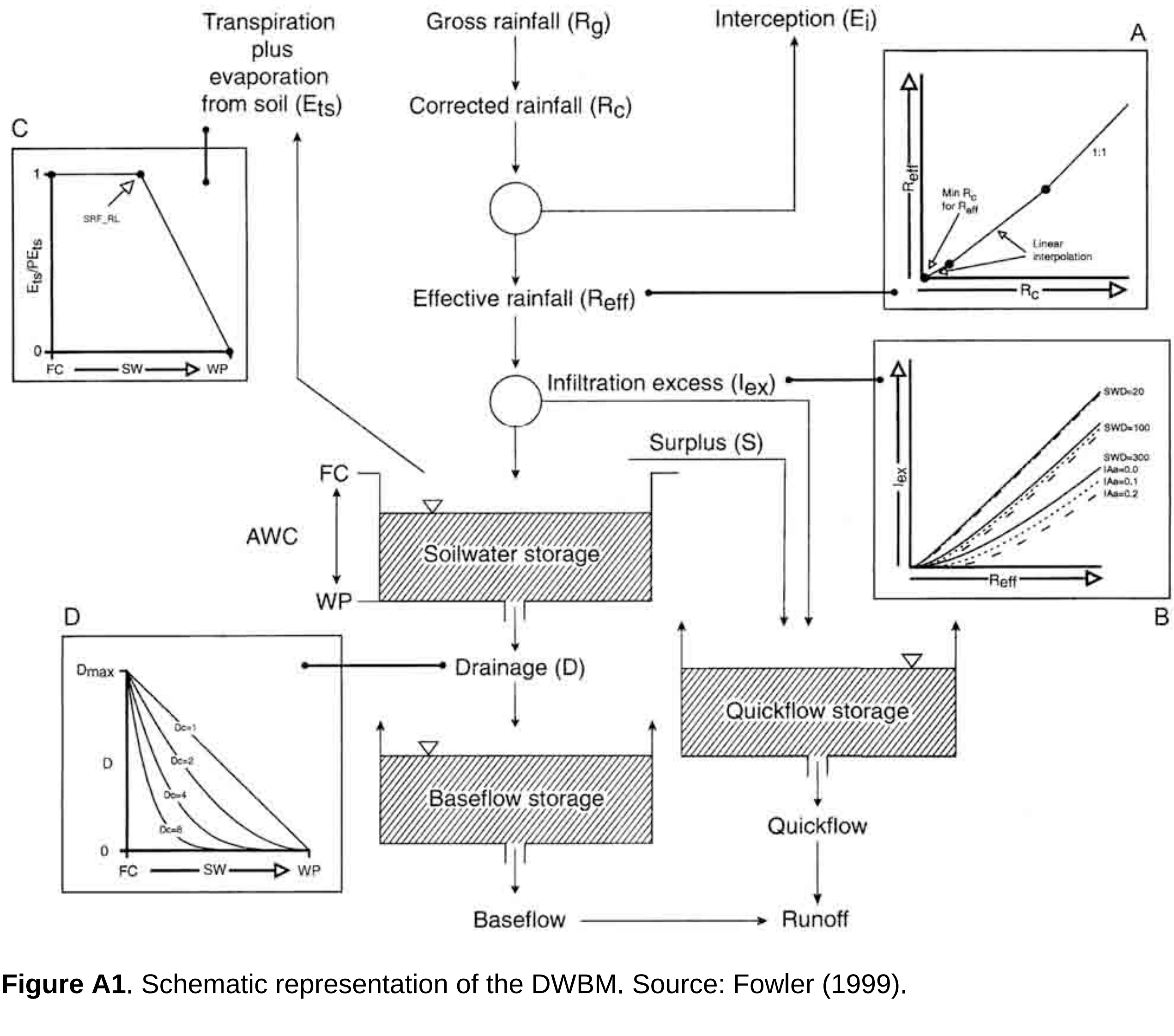

Figure A1. Schematic representation of the DWBM. Source: Fowler (1999).

R_{eff} is then partitioned between infiltration and infiltration excess (I_{ex}). I_{ex} is calculated using a modified version of the 'SCS curve number method' (USDA 1972), and is a function of R_{eff} , the soil water deficit (SWD), surface storage capacity (SSC, #6) and an 'initial abstraction' parameter (IA_a, #7), which represents how effectively available storage capacity is utilised. Inset B shows examples of the resulting curve 'families'. The net effect is that significant I_{ex} requires wet soils (low SWD) and/or heavy precipitation. I_{ex} is routed to a slow-release baseflow runoff store.

Soil water storage is defined in terms of available water capacity (AWC, #8), the difference between field capacity (FC) and wilting point (WP). There is provision for a pseudo upper soil layer (AWCup, #9) which fills and empties first, the latter at the potential rate. This is included to allow for relatively high evaporation from a dry soil immediately after a rainfall event. Input to soil water storage is simply R_{eff} minus I_{ex}. Outputs are drainage to groundwater, evaporation (excluding E_i), and surplus water when FC has been reached.

Drainage (D) is modelled as a non-linear function of soil water content (Inset D), based on Aston and Dunin (1977), and is controlled by two parameters. The maximum drainage rate (D_{max}, #10) prescribes the drainage flux at FC (drainage for soils between FC and saturation is handled by 'surplus' – see below). The second parameter (D_c, #11) defines the shape of the drainage decay curve as the soil dries. D is routed to a slow-release baseflow runoff store.

Evaporation (E_{ts}[8]), is calculated as a function of potential dry canopy evaporation (PE_{ts}[9]) and soil water content. E_{ts} is equal to PE_{ts} at FC and is zero at WP (E_{ts}/PE_{ts} = 1 and 0 respectively). At intermediate soil water contents E_{ts} is modelled as a two-phase process: $E_{ts}=PE_{ts}$ from FC to a user-defined soil water content (SRF_RL, #12), then linear decay of E_{ts}/PE_{ts} from SRF_RL to WP. The resulting non-linear relationship (Inset C) is based on the recommendation of Baier et al. (1979) for medium-textured, non-irrigated soils and has been demonstrated to work well for New Zealand conditions (e.g. Parfitt et al. 1985a,b).

The DWBM is designed to be applicable for different vegetation covers. It therefore has three parameters (PEtsPEg0, PEtsPEg5, EiPEts, #13 – # 15) that deal with the fact that, although there are important differences in the character of evaporation with vegetation type, PE is routinely measured over grass. For pasture, these parameters all default to one, because PE_g is an acceptable approximation for PE_{ts} for short crops (McNaughton and Jarvis 1983). The modelling implications are that $PE_{ts}=PE_g$ and that Ei reduces PE_{ts} mm for mm.

Surplus (S) is a pooled flux representing rapid drainage from soils between saturation and FC, plus any additional infiltration excess when soil water content reaches saturation. S is affected by all parameters that control soil water storage and fluxes and can reasonably viewed as a pooled residual flux (requiring no additional parameters). S is routed to a quick-release quickflow runoff store.

The lower two stores in Figure A1 relate to runoff. Both are limitless stores that represent water in the catchment available for runoff, but in locations with different pathways to the channel. Each store is emptied using a two-parameter recession curve equation (Boughton 1986), with parameter values set to simulate the quickflow (QQa, QQb, #16, #17) and baseflow (QBa, QBb, #19, #20) components of the hydrograph. QQprop (#18) is an additional quickflow parameter that prescribes the maximum proportion of the quickflow store that can be emptied in one day. Note that none of these parameters affects the soil water balance – they merely control the shape of the hydrograph.

---

[8] Because free-water evaporation (interception) is treated separately, modelled evaporation from the soil is transpiration (t) and diffusion of water directly from the soil (s). Hence the use of the E_{ts} term.

[9] PE_{ts} is derived from standard PE calculations from measurements over grass.

Table A1. DWBM parameters

#	Parameter	Units	Default	Details
1	INT0P	mm	0.2	*Effective rainfall threshold*. Minimum R_c for P_{eff}.
2	INT1P	mm	3.0	*Interception hinge point 1 x-axis value.* Paired with INT1Peff.
3	INT1Peff	mm	2.1	*Interception hinge point 1 y-axis value.* Paired with INT1P.
4	INT2P	mm	10.0	*Interception hinge point 2 x-axis value.* Paired with INT2Peff.
5	INT2Peff	mm	8.5	*Interception hinge point 2 y-axis value.* Paired with INT2P.
6	SSC	mm	1.0	*Surface storage capacity*. Used to calculate I_{ex} (which decreases as SSC increases).
7	IAa	-	0.1	*Initial abstraction parameter*. Dimensionless parameter representing how effectively available soil storage capacity is utilised. 0–1 range, but values above 0.2 unlikely. Used to calculate I_{ex} (which decreases as IAa increases).
8	AWC	mm	100	*Available water capacity*. Soil water storage capacity in the rooting zone.
9	AWCup	mm	0	*Available water capacity upper layer*. Pseudo upper soil layer to which any input is initially routed and which empties by evaporation first (at the potential rate).
10	Dmax	mm	1.0	*Drainage at field capacity*. Drainage of soil water when soil water storage is at FC (SWD=0).
11	Dc	-	10.0	*Drainage curve decay parameter*. Dimensionless parameter controlling the shape of the drainage decay curve from FC (Dmax) to WP (0). 1–30 range. Higher values reduce D more quickly as soil dries.
12	SRF_RL	%	50.0	*Soil resistance factor reduction level*. Soil water content (%) at which the soil resistance factor begins to decline linearly to zero at WP (E_{ts} = SRF x PE_{ts}).
13	PEtsPEg0	ratio	1.0	*Ratio of PE_{ts} to PE_g at small values of PE_g. PE_{ts}/PE_g* at PE_g=0. Used, with PEtsPEg5 when PE_{ts} for the vegetation cover differs from PE_g (default is 1.0 for pasture).
14	PEtsPEg5	ratio	1.0	*Ratio of PE_{ts} to PE_g at large values of PE_g. PE_{ts}/PE_g* at PE_g=5. Used, with PEtsPEg0 when PE_{ts} for the vegetation cover differs from PE_g (default is 1.0 for pasture). NB: two parameters used because the ratio may be PE_g-dependent.
15	EiPEts	ratio	1.0	*Ratio of E_i to PE_{ts}*. Reduction of PE_{ts} for each mm of E_i (default is 1.0 for pasture).
16	QQa	-	3.0	*Quickflow store depletion parameter a*. Dimensionless parameter in the equation used to deplete the quickflow store (Quickflow = $Store^{QQb}/QQa$). Paired with QQb.
17	QQb	-	1.0	*Quickflow store depletion parameter b*. Dimensionless parameter in the equation used to deplete the quickflow store (Quickflow = $Store^{QQb}/QQa$). Paired with QQa.
18	QQprop	ratio	0.8	*Maximum daily quickflow store depletion*. Maximum proportion of quickflow store that can be depleted in one day.
19	QBa	-	130.0	*Baseflow store depletion parameter a*. Dimensionless parameter in the equation used to deplete the baseflow store (Baseflow = $Store^{QBb}/QBa$). Paired with QBb.
20	QBb	-	1.15	*Baseflow store depletion parameter b*. Dimensionless parameter in the equation used to deplete the baseflow store (Baseflow = $Store^{QBb}/QBa$). Paired with QBa.

7.2. Daily water balance model use guide

The following three files are needed to run the DWBM:

1. **dwbm08.jar**. The daily water balance program.

2. **dwbm_parameters.csv**. Text file containing model parameter values (e.g. storage capacity volumes and values controlling movement of water between stores).

3. **dwbm_in.csv**. Text file of daily P and PE data used to drive the model.

The '.csv' at the end of the two text files stands for 'comma-separated values'. Excel can read and write this format.

Create 'dwbm_in.csv' for the site in question, ensuring that there are exactly three header lines and that the file is saved in csv format. Below is an example snippet from a correctly formatted file.

```
Auckland 1900-1998: homog. P & modelled PE (6th order poly. on AA cum. monthly PE).  22 missing P replaced with zeros.,,,,
Homogenised P from Salinger (June 2002) & modelled PE (6th order polynomial on AA cumulative monthly PE) from Fowler (2002),,,,
Year,Month,Day,Rc,PEg
1900,9,1,10.1,2.2
1900,9,2,18.4,2.2
1900,9,3,14.4,2.2
1900,9,4,10.1,2.3
1900,9,5,1.5,2.3
1900,9,6,0.6,2.3
1900,9,7,0,2.3
```

'dwbm_parameters.csv' can be edited using a text editor, but can also be done by saving parameter settings when running the model (recommended).

All files must be in the same directory/folder for the model to run successfully.

To run the program a 'double-click' on dwbm08.jar will often suffice[10]. Otherwise, follow instructions for the Java runtime environment.

On start-up the user is presented with a screen that looks similar to Figure 3, but with empty graphs. If required input files are present and correctly formatted, the text box at the bottom of the screen will display something similar to below, indicating progress.

```
Default parameters file ('dwbm_parameters.csv') found
Parameters read & text fields updated
Default input file (dwbm_in.csv) found
Reading data (dwbm_in.csv)
Site: Napier 1932-2008: modelled PE (6th order poly. on cum. monthly PE).
1932.1.1 - 2008.1.1
Done
```

Program operation is handled through a typical graphical interface.

Note that after reading 'dwbm_parameters.csv' the fields on the left of the screen are updated. These text fields are editable and the values can be saved back into 'dwbm_parameters.csv' ('Save as default' menu item), or to another file.

[10] dwbm08.jar is a Java Archive file. The program should run on any computer with a Java runtime environment (JRE) installed.

There are 24 text fields, but only 20 parameters are listed in Table A1. The four missing 'parameters' are actually starting store values (SWD0, SWup0) or fluxes (QQ0, QB0). SWD0 (starting SWD) should be changed to something sensible for the start month (and never more than AWC). The default values for the others are probably fine.

Most parameter values have relevant units, making selection choice relatively straight forward. Some have suggested ranges in Table A1. Indiscriminate adjustment of parameters is unwise and the results unpredictable. The DWBM was developed as a research tool and does not (yet) have error checking code.

The 'Run' menu has two options. On first run with a new data set the 'Standard Water Balance' option should be selected first. Doing so should produce a result similar to Figure 3 with something like the following in the text box:

```
Starting water balance calculations
Water balance calculations completed normally
Means (mm/day): Rc = 2.43, PEg = 2.66, E = 1.67 (0.33 + 1.33), Q = 0.77
Mean SWD (mm): = 54.52. Runoff ratio = 0.32
Graphing data
Calculating & writing monthly statistics
FINISHED
```

The first two lines indicate that operation proceeded normally to completion. The third and fourth give some overall statistics (the terms in brackets are E_i and E_{ts}, Q is runoff). The monthly statistics referred to in the sixth line are written to two files ('dwbm_out_month_by_year_matrix.csv', 'dwbm_out_monthly_series.csv'). These contain monthly means (mm/day) for four key simulation variables (SWD, E, E_{ts}, Q). The files hold identical information, but format it differently. A third file ('dwbm_out.csv') is also written at this time. This file lists headers, parameters, and daily simulation results.

The second 'Run' option ('Response Surface Analysis') does all of the above, then launches into multiple reruns of the model with incremental adjustments to P and PE_g. It erases the previous information (this is why an initial simple water balance run is advisable), producing the following text messages when complete.

```
Response surface calculations
RcScale = 1.5, PEgScale = 1.5
Response surface calculations completed normally
Writing response surface results
FINISHED
```

Note that the second line shows runtime incremental adjustments to RcScale and PEgScale (1.5 values are the end points). A further six output files are written, each titled similarly to 'dwbm_out_rs_Ets.csv', where the output variable is in the file name (here E_{ts}).

The snippet below is the beginning of 'dwbm_out_rs_Ets.csv' (after importing the file into Excel). It shows the mean E_{ts} for January (mm/day), calculated over all January days. The -50 to 50 values in the first column and row of the matrix refer to percentage adjustments to PE_g and R_c (RcScale 1.5 above is 50 here). This is the data used to plot the response surfaces. The tabled value at 0,0 (1.5403) is the mean E_{ts} for the model run with no adjustments. Similar tables are produced for each month, each season, and annual.

MEAN Ets JAN (mm/day)											
PEg\Rc	-50	-40	-30	-20	-10	0	10	20	30	40	50
50	0.7887	0.9503	1.1084	1.2612	1.41	1.5546	1.6937	1.8275	1.9559	2.0781	2.1952
40	0.7872	0.9485	1.106	1.2583	1.4069	1.5509	1.6888	1.8212	1.9481	2.0685	2.1838
30	0.7856	0.9467	1.1037	1.2556	1.4035	1.5466	1.6833	1.8147	1.9394	2.0581	2.1715
20	0.7844	0.9447	1.1016	1.253	1.4004	1.5427	1.6786	1.8079	1.9307	2.0475	2.1585
10	0.7832	0.9439	1.1004	1.2515	1.399	1.5406	1.6747	1.8017	1.9226	2.0365	2.1442
0	0.7827	0.9444	1.1007	1.2523	1.3998	1.5403	1.6721	1.7969	1.9144	2.0244	2.1278
-10	0.7849	0.9475	1.1045	1.2575	1.4048	1.5431	1.6722	1.7925	1.905	2.0094	2.1067
-20	0.7917	0.9565	1.1162	1.2704	1.4163	1.5507	1.674	1.7877	1.8928	1.9897	2.0798
-30	0.8076	0.9786	1.1415	1.2951	1.4355	1.5608	1.6744	1.7788	1.8742	1.9619	2.0421
-40	0.8441	1.0212	1.1836	1.3281	1.454	1.5656	1.6665	1.7566	1.8372	1.9095	1.9732
-50	0.9091	1.0824	1.2293	1.351	1.4559	1.5458	1.6239	1.6901	1.7444	1.787	1.8199

The same data is also written in an alternative ‘xyz’ list format (snippet below). This may be a more convenient form for some graphing software applications.

Rc	PEg	JAN	FEB	MAR	APR	MAY	JUN	JUL	AUG	SEP	OCT	NOV	DEC	DJF	MAM	JJA	SON	ANN
-50	-50	0.9091	0.7711	0.6960	0.5166	0.3486	0.2330	0.2595	0.4854	0.8780	1.3223	1.3827	1.1430	0.9411	0.5204	0.3260	1.1943	0.7454
-50	-40	0.8441	0.7864	0.7264	0.5705	0.4069	0.2852	0.3190	0.5999	1.0740	1.4768	1.3339	1.0311	0.8872	0.5679	0.4014	1.2949	0.7879
-50	-30	0.8076	0.8081	0.7558	0.6155	0.4597	0.3345	0.3800	0.7147	1.2465	1.5362	1.2250	0.9364	0.8507	0.6103	0.4764	1.3359	0.8183
-50	-20	0.7917	0.8294	0.7856	0.6520	0.5040	0.3809	0.4413	0.8254	1.3824	1.5267	1.1056	0.8752	0.8321	0.6472	0.5492	1.3383	0.8417
-50	-10	0.7849	0.8486	0.8129	0.6833	0.5402	0.4247	0.5010	0.9289	1.4810	1.4714	1.0011	0.8402	0.8246	0.6788	0.6182	1.3178	0.8598
-50	0	0.7827	0.8652	0.8355	0.7095	0.5721	0.4648	0.5593	1.0250	1.5415	1.3904	0.9188	0.8226	0.8235	0.7057	0.6831	1.2836	0.8740
-50	10	0.7832	0.8800	0.8541	0.7310	0.6011	0.5020	0.6138	1.1120	1.5686	1.3020	0.8574	0.8151	0.8261	0.7287	0.7426	1.2427	0.8850
-50	20	0.7844	0.8937	0.8686	0.7491	0.6284	0.5376	0.6663	1.1883	1.5704	1.2147	0.8141	0.8136	0.8306	0.7487	0.7974	1.1998	0.8941
-50	30	0.7856	0.9058	0.8811	0.7651	0.6538	0.5699	0.7152	1.2556	1.5550	1.1335	0.7840	0.8153	0.8356	0.7667	0.8469	1.1575	0.9017
-50	40	0.7872	0.9165	0.8923	0.7792	0.6765	0.5999	0.7616	1.3126	1.5262	1.0629	0.7636	0.8184	0.8407	0.7827	0.8913	1.1176	0.9081
-50	50	0.7887	0.9260	0.9020	0.7910	0.6972	0.6288	0.8047	1.3602	1.4869	1.0039	0.7507	0.8228	0.8458	0.7967	0.9312	1.0805	0.9136
-40	-50	1.0824	0.8937	0.7827	0.5593	0.3549	0.2319	0.2560	0.4768	0.8641	1.3386	1.5139	1.3296	1.1019	0.5657	0.3215	1.2389	0.8070
-40	-40	1.0212	0.9121	0.8329	0.6243	0.4208	0.2835	0.3152	0.5890	1.0668	1.5648	1.5328	1.2470	1.0601	0.6260	0.3959	1.3882	0.8675
-40	-30	0.9786	0.9385	0.8770	0.6803	0.4810	0.3355	0.3755	0.7048	1.2662	1.6990	1.4635	1.1528	1.0233	0.6794	0.4719	1.4762	0.9127
-40	-20	0.9565	0.9676	0.9143	0.7274	0.5362	0.385	0.4369	0.8223	1.4475	1.7443	1.3559	1.0785	1.0009	0.726	0.5481	1.5159	0.9477
-40	-10	0.9475	0.9937	0.9465	0.7691	0.5815	0.4336	0.4987	0.939	1.5934	1.7306	1.2451	1.0325	0.9912	0.7657	0.6238	1.5231	0.9759

7.3. DWBM parameter sensitivity analysis

Table A2 shows the sensitivity of DWBM summary output variables to a subset of 11 of the 20 parameters listed in Table A1. The missing nine parameters are:

- all five runoff parameters, because runoff is not relevant to this application of the model;
- two interception parameters (INT1P, INT2P), because they are respectively paired with INT1Peff and INT2Peff and changing one of each pair is sufficient; and,
- PEtsPEg0 and PEtsPEg5, because these two parameters are primarily intended to deal with non-pasture contexts.

To analyse the sensitivity of the DWBM, all parameters were set to the default values listed in Table A1. Then, working through each parameter in turn, adjustments were made to the parameter and the impact on summary statistics (E, E_i, E_{ts}, SWD, percent runoff) was noted. Alternative parameter values either side of the default were tested in nine cases, using a plausible range (based on expert judgement). This was not possible for AWCup or EiPEts, because in these two cases the default values are lower limits - AWCup cannot be less than zero and a value less than one for EiPEts is implausible for pasture. In these two cases, two alternative parameter values are still tested, both higher than the default.

In addition to the individual parameter analysis, results are tabled for an additional sensitivity analysis. This involved ‘turning off’ interception by setting several interception parameter values to ensure that all P contributes to P_{eff}. This degrades the DWBM to a cruder approach, where all evaporation is combined, with no attempt to distinguish between different evaporation pathways. This experiment was done to test if including an empirical interception function (yielding R_{eff}) gave a materially different result.

Interception (INT0P, INT1Peff, INT2Peff). E_i is notably sensitive to adjustments to the interception parameters. Adjusting INT0P had the least affect (≤7%), but the changes to INT1Peff and INT2Peff resulted in impacts of 15-27%. The bulk of changes in E_i were compensated for by inverse impacts on E_{ts} (≤4%)[11] with negligible net impacts on E (≤1%), and therefore on soil water content and runoff. Conjoint changes to the three parameters to *minimise* E_i (INT0P = 0.1, INT1Peff = 2.5, INT2Peff = 9) resulted in a 45% reduction in E_i, with an 8% compensating increase in E_{ts}, and 3% net decrease in E.

[11] Percentage change are much lower for E_{ts} because the flux is about a factor of four larger than E_i.

Table A2. DWBM sensitivity analysis for selected parameters. Model sensitivity was assessed using mean values (1932-2007) for summary variables representing evaporation (E, E_i, E_{ts}), the soil water regime (SWD), and water balance partitioning between evaporation and runoff (represented by Runoff (%)). Initial run results are for default values (2nd column). For each parameter, the simulation was re-run with only the listed parameter value (3rd column) changed. An exception is the "Interception off" simulation where several parameters were adjusted. SWD results are not shown for adjustments to AWC because a simple comparison is not meaningful.

Parameter	Initial value	Selected value	E (E_i + E_{ts}) (mm/day)	SWD (mm)	Runoff (%)
Initial run			**1.633 (0.333 + 1.300)**	**50.947**	**32.9**
INT0P (mm)	**0.2**	0.1	1.633 (0.326 + 1.307)	50.917	32.9
		0.5	1.634 (0.357 + 1.277)	51.037	32.8
INT1Peff (mm)	**2.1**	1.5	1.652 (0.410 + 1.242)	51.449	32.1
		2.5	1.626 (0.282 + 1.343)	50.739	33.2
INT2Peff (mm)	**8.15**	7.5	1.669 (0.403 + 1.267)	51.206	31.4
		9	1.595 (0.243 + 1.352)	50.877	34.4
SSC (mm)	**1**	0	1.624 (0.333 + 1.291)	51.543	33.2
		2	1.640 (0.333 + 1.307)	50.502	32.6
IAa	**0.1**	0	1.570 (0.333 + 1.236)	53.401	35.5
		0.2	1.662 (0.333 + 1.329)	49.639	31.6
AWC (mm)	**100**	50	1.445 (0.333 + 1.111)	-	40.6
		200	1.865 (0.333 + 1.532)	-	23.4
AWCup (mm)	**0**	10	1.665 (0.333 + 1.332)	54.530	31.5
		20	1.678 (0.333 + 1.345)	55.814	31.0
Dmax (mm)	**1**	0.5	1.640 (0.333 + 1.307)	49.968	32.6
		3	1.615 (0.333 + 1.282)	53.438	33.6
Dc	**10**	5	1.616 (0.333 + 1.283)	52.518	33.6
		20	1.642 (0.333 + 1.308)	49.962	32.5
SRF_RL (%)	**50**	20	1.564 (0.333 + 1.231)	43.861	35.7
		80	1.683 (0.333 + 1.349)	56.866	30.8
EiPEts	**1**	1.2	1.647 (0.333 + 1.314)	51.553	32.3
		1.5	1.664 (0.333 + 1.331)	52.217	31.6
Interception off*			1.571 (0.000 + 1.571)	50.864	35.4

* INT0P = 0, INT1P & INT1Peff = 3, INT2P & INT2Peff = 10.

Infiltration (SSC, IAa). Adjustments to the infiltration parameters affect how much P_{eff} enters into soil water storage. This in turn affects E_{ts}, SWD, and surface runoff. The sensitivity analysis indicates that output is insensitive to plausible changes to SSC. Changes to IAa, particularly the reduction to zero, had up to a 5% impact on E_{ts}, with associated impacts on soil dryness and runoff.

Soil water (AWC, AWCup). Increasing soil water storage capacity (higher AWC) increases the capacity of the soil to accommodate precipitation inputs. Water is therefore more readily available to meet evaporative demand and, because soil water content is less frequently near capacity, D and I_{ex} are both reduced. The net result is that AWC is the parameter that model output is most sensitive to. For example, increasing AWC from 100 to 200 mm results in an 18% increase in E_{ts} (at the expense of runoff). Adding an upper soil layer to the model (AWCup > 0) also slightly increases E_{ts} (≤3%).

Drainage (Dmax, Dc). Model output is insensitive to adjustments to both drainage parameters (≤1% impacts on both E and E_{ts}).

Evaporation (SRF_RL, EiPEts). Model output is moderately sensitive to adjustments in SRF_RL, with net impacts on E_{ts} and E of -5–4% and -4–3% respectively. Sensitivity is greatest in shoulder seasons when SWDs are more frequently at the intermediate values where the parameter change is influential. Sensitivity to EiPEts is low (≤1% impacts on both E and E_{ts}).

Interception off. Adjusting the interception parameter values to 'turn off' interception implements the assumption that it is reasonable to lump all forms of evaporation from a pasture surface together. Thus, the E_{ts} flux actually becomes E and the relevant sensitivity results also relate to E. Turning off interception increases R_{eff} by 15.7%. This in turn increases I_{ex}, reducing soil water recharge and increasing runoff, especially over the winter months when SWDs are low. Simulated E is lower in all months (by 0.3 – 3.0% from August through April and by 8.6 – 17.6% from May through July, though off a much lower baseline E) and by 3.8% overall. Although E is lower, SWDs are also slightly lower for nine months (November – July), due to more than compensating reduced soil water recharge, noted above. Overall there is a widening of the inter-monthly E range, but this is minor over the pasture growing season, and no shift in the seasonal cycle is evident.